14. Obi T, Nishioka K, Ross OA, et al. Clinicopathologic study of a SNCA gene duplication patient with Parkinson disease and dementia. Neurology 2008;70:238–241.
15. Muenter MD, Forno LS, Hornykiewicz O, et al. Hereditary form of parkinsonism—dementia. Ann Neurol 1998;43:768–781.
16. Gwinn-Hardy K, Mehta ND, Farrer M, et al. Distinctive neuropathology revealed by alpha-synuclein antibodies in hereditary parkinsonism and dementia linked to chromosome 4p. Acta Neuropathol (Berl) 2000;99:663–672.
17. Hughes AJ, Daniel SE, Kilford L, Lees AJ. Accuracy of clinical diagnosis of idiopathic Parkinson's disease: a clinico-pathological study of 100 cases. J Neurol Neurosurg Psychiatry 1992;55:181–184.
18. Miller SA, Dykes DD, Polesky HF. A simple salting out procedure for extracting DNA from human nucleated cells. Nucleic Acids Res 1988;16:1215.
19. Ishibashi K, Ishii K, Oda K, Kawasaki K, Mizusawa H, Ishiwata K. Regional analysis of age-related decline in dopamine transporters and dopamine D2-like receptors in human striatum. Synapse 2009;63:282–290.
20. American Academy of Sleep Medicine. International classification of sleep disorders, revised: diagnostic and coding manual. Rochester, MN: American Academy of Sleep Medicine; 2001.
21. Rechtschaffen A, Kales A. A manual of standardized terminology, techniques and scoring system for sleep stages of human subjects, public health service. Washington, DC: U.S. Government Printing Office; 1968.
22. Lapierre O, Montplaisir J. Polysomnographic features of REM sleep behavior disorder: development of a scoring method. Neurology 1992;42:1371–1374.
23. Stiasny-Kolster K, Clever SC, Moller JC, Oertel WH, Mayer G. Olfactory dysfunction in patients with narcolepsy with and without REM sleep behaviour disorder. Brain 2007:130 (Part 2):442–449.
24. Katotomichelakis M, Balatsouras D, Tripsianis G, Tsaroucha A, Homsioglou E, Danielides V. Normative values of olfactory function testing using the "sniffin" sticks'. Laryngoscope 2007;117:114–120.
25. Hummel T, Sekinger B, Wolf SR, Pauli E, Kobal G. "Sniffin" sticks': olfactory performance assessed by the combined testing of odor identification, odor discrimination and olfactory threshold. Chem Senses 1997;22:39–52.
26. Iranzo A, Molinuevo JL, Santamaria J, et al. Rapid-eye-movement sleep behaviour disorder as an early marker for a neurodegenerative disorder: a descriptive study. Lancet Neurol 2006; 5:572–577.
27. Farrer MJ. Genetics of Parkinson disease: paradigm shifts and future prospects. Nat Rev Genet 2006;7:306–318.
28. Aarsland D, Ballard C, Larsen JP, McKeith I. A comparative study of psychiatric symptoms in dementia with Lewy bodies and Parkinson's disease with and without dementia. Int J Geriatr psychiatry 2001;16:528–536.
29. Emre M, Aarsland D, Brown R, et al. Clinical diagnostic criteria for dementia associated with Parkinson's disease. Mov Disord 2007;22:1689–1707; quiz1837.
30. Puschmann A, Wszolek ZK, Farrer M, Gustafson L, Widner H, Nilsson C. Alpha-synuclein multiplications with parkinsonism, dementia or progressive myoclonus? Parkinsonism Relat Disord 2009;15:390–392.
31. Braak H, Rub U, Gai WP, Del Tredici K. Idiopathic Parkinson's disease: possible routes by which vulnerable neuronal types may be subject to neuroinvasion by an unknown pathogen. J Neural Transm 2003;110:517–536.
32. Albin RL, Minoshima S, D'Amato CJ, Frey KA, Kuhl DA, Sima AA. Fluoro-deoxyglucose positron emission tomography in diffuse Lewy body disease. Neurology 1996;47:462–466.
33. Ishii K, Imamura T, Sasaki M, et al. Regional cerebral glucose metabolism in dementia with Lewy bodies and Alzheimer's disease. Neurology 1998;51:125–130.
34. Lobotesis K, Fenwick JD, Phipps A, et al. Occipital hypoperfusion on SPECT in dementia with Lewy bodies but not AD. Neurology 2001;56:643–649.

SYNAPSE 63:282–290 (2009)

Regional Analysis of Age-Related Decline in Dopamine Transporters and Dopamine D_2-Like Receptors in Human Striatum

KENJI ISHIBASHI,[1,2] KENJI ISHII,[1]* KEIICHI ODA,[1] KEIICHI KAWASAKI,[1] HIDEHIRO MIZUSAWA,[2] AND KIICHI ISHIWATA[1]

[1]*Positron Medical Center, Tokyo Metropolitan Institute of Gerontology, Tokyo 173-0022, Japan*

[2]*Department of Neurology and Neurological Science, Graduate School, Tokyo Medical and Dental University, Tokyo 113-8519, Japan*

KEY WORDS aging; dopamine; PET; CFT; raclopride

ABSTRACT The purpose of this study was to evaluate the mechanisms of age-related decline of dopamine transporter (DAT) and dopamine D_2-like receptor (D_2R) densities in the human striatum by focusing on regional difference. Methods: Positron emission tomography (PET) with [^{11}C]CFT and [^{11}C]raclopride for measuring DATs and D_2Rs, respectively, was performed on 16 healthy volunteers ranging from 21 to 74 years in age. To evaluate in detail the regional difference within the striatum, in addition to the conventional region-of-interest-based analysis, we created a parametric image that enabled us to visualize the regional decline rate on a voxel-by-voxel basis, mapping the slope of the regression line between the age and uptake index of each tracer. Results: The decreasing rates corresponded to 6.1, 5.5, and 5.6% per decade for DATs and 5.8, 4.9, and 4.8% per decade for D_2Rs in the caudate nucleus, anterior putamen, and posterior putamen, respectively. The caudate nucleus for both DATs and D_2Rs were the fastest among the striatum, and the regional difference of the decreasing rate for DATs was consistently associated with that for D_2Rs. Meanwhile, previous histological studies have shown that age-related cell loss in the substantia nigra is likely to preferentially affect its dorsomedial part, which projects to the caudate nucleus. Conclusions: These results suggested that neuronal cell loss in the substantia nigra may be associated with the age-related DAT decline, and DAT decline may be associated functionally with age-related D_2R decline. **Synapse 63:282–290, 2009.**

INTRODUCTION

Numerous neuroimaging studies in vivo (Ishikawa et al., 1996; Kazumata et al., 1998; Pirker et al., 2000; Pohjalainen et al., 1998; Rinne et al., 1993; Rinne et al., 1998; van Dyck et al., 1995; Volkow et al., 1994; Volkow et al., 1996a; Volkow et al., 1996b; Volkow et al., 1998; Wong et al., 1988; Wong et al., 1997) and neurobiological studies in vitro (Allard and Marcusson, 1989; De Keyser et al., 1990; Rinne, 1987; Rinne et al., 1990; Seeman et al., 1987; Severson et al., 1982; Zelnik et al., 1986) have consistently demonstrated a significant age-related decrease in dopamine transporter (DAT) density as a maker of presynaptic function and dopamine D_2-like receptor (D_2R) density as a marker of postsynaptic function. The precise mechanism of the decline is not clear yet; however, it is probably related to neuronal cell loss and/or functional changes of the remaining cells. Volkow et al. (1998) measured both presynaptic and postsynaptic markers simultaneously in humans to evaluate age-related effects by PET. They showed that the association between DATs and D_2Rs was independent of age and suggested that the expression of receptors and transporters with age may be driven by functional changes in the synapse rather than by neuronal cell loss. However, many histological studies have shown a decrease in the number of neurons in the substantia nigra (Fearnley and Lees, 1991; Gibb and Lees, 1991; Stark and Pakkenberg, 2004). From these reports, we speculated that neuronal cell loss in the substantia nigra was significantly related to the age-related decline of DAT density, in addition to the association between DATs and D_2Rs. Thus, we

*Correspondence to: Kenji Ishii, Positron Medical Center, Tokyo Metropolitan Institute of Gerontology, 1-1 Nakacho, Itabashi-ku, Tokyo 173-0022, Japan. E-mail: ishii@pet.tmig.or.jp

Received 4 March 2008; Accepted 31 July 2008

DOI 10.1002/syn.20603

Published online in Wiley InterScience (www.interscience.wiley.com).

postulated that if neuronal cell loss in the substantia nigra is associated with age-related DAT decline in the striatum, the regional distribution of cell loss in the substantia nigra should be associated with the regional distribution of age-related DAT decline in the striatum. This is because cells in the substantia nigra project to the striatum with a regionally corresponding arrangement. Further, if age-related DAT decline is associated functionally with age-related D_2R decline, the regional distribution of the age-related decreasing rate of DATs should be associated with that of D_2Rs in the striatum, because presynaptic terminals are adjacent to postsynaptic neurons.

To examine this hypothesis, we focused on investigating the regional difference in the age-related deceasing rates. We divided the striatum into three regions-caudate nucleus, anterior putamen, and posterior putamen. We then investigated the age-related changes and the association between DATs and D_2Rs for each region in the same subject by PET. Additionally, to visually evaluate the detailed regional differences in the deceasing rate of each marker, we developed a new imaging technique to create a decay image that maps the slope of the regression line on a voxel-by-voxel basis.

MATERIALS AND METHODS

Subjects

A total of 16 healthy volunteers (15 men and 3 women), ages 21–74 years (mean age = 42.3, SD = 21.1), participated in this study. All subjects were right-handed. They were deemed healthy based on their medical history, physical and neurological examinations by neurologists, and magnetic resonance imaging (MRI) of the brain evaluated by radiologists. None of them was on medication at the time of the study. This study protocol was approved by the Ethics Committee of the Tokyo Metropolitan Institute of Gerontology. Written informed consent was obtained from all participants.

PET imaging

PET studies were performed at the Positron Medical Center, Tokyo Metropolitan Institute of Gerontology using a SET 2400W scanner (Shimadzu, Kyoto, Japan) in the three-dimensional scanning mode (Fujiwara et al., 1997). Carbon-11-labeled 2β-carbomethoxy-3β-(4-fluorophenyl)-tropane ([^{11}C]CFT) and Carbon-11-labeled raclopride ([^{11}C]raclopride) were prepared as described previously (Kawamura et al., 2003; Langer O, 1999). All subjects underwent the two PET studies on the same day. Each subject received an intravenous bolus injection of 352 ± 49 (mean ± SD) MBq of [^{11}C]CFT. Then, 2.5–3 h after the injection of [^{11}C]CFT, each subject received an intravenous bolus injection of 322 ± 48 (mean ± SD) MBq of [^{11}C]raclopride. To estimate the binding potentials, for 5 of 16 subjects, dynamic scans were performed for 90 min with [^{11}C]CFT and for 60 min with [^{11}C]raclopride. To measure the uptake of these two tracers, for the remaining 11 subjects, static scans were performed for 75–90 min after the injection of [^{11}C]CFT and for 40–55 min after the injection of [^{11}C]raclopride, respectively. The specific activity at the time of injection ranged from 12.4 to 119.6 GBq/μmol for [^{11}C]CFT and from 14.0 to 188.0 GBq/μmol for [^{11}C]raclopride. The transmission data were acquired using a rotating ^{68}Ga/^{68}Ge rod source for attenuation correction. The images consist of 2 × 2 × 3.125 mm^3 voxels with a 128 × 128 matrix and 50 slices.

MR imaging

High-resolution MRI was obtained using a 1.5-Tesla Signa EXCITE HD scanner (GE, Milwaukee, WI) in the three-dimensional mode (3DSPGR; echo time: 2.3 ms, repetition time: 18 ms), which provided 124 contiguous slices with a matrix size of 256 × 256, pixel size of 0.9375 × 0.9375 mm^2, and slice thickness of 1.3 mm.

Data analysis

Uptake ratio index on region-of-interest basis

Image manipulations were carried out by using a medical image processing application package "Dr View/LINUX" version R2.0 (AJS, Tokyo, Japan) and SPM2 (The Wellcome Department of Imaging Neuroscience, Institute of Neurology, University College London, London, UK) implemented in MATLAB version 7.0.1 (MathWorks,. Natick, MA).

Circular regions of interest (ROIs) were placed with reference to the brain atlas and individually coregistered MRI by SPM2: one region of interest (ROI) with 6-mm diameter was placed on the caudate, two ROIs on the anterior putamen and two ROIs on the posterior putamen to contain the most intense activity on both the left and right sides in each of the two contiguous slices. Each ROI in the striatum was estimated smaller enough based on the actual structure of MRI to minimize resolution-induced problem with ill-defined edges. A total of 50 ROIs with 10-mm diameter were placed throughout the cerebellar cortex in five contiguous slices.

To evaluate the uptake of [^{11}C]CFT and [^{11}C]raclopride, we calculated the uptake ratio index by the following formula (Antonini et al., 1993; Frost et al., 1993; Wong et al., 1993).

$$\text{Uptake Ratio Index} = \frac{(\text{Activity}_{\text{Region}} - \text{Activity}_{\text{Cerebellum}})}{\text{Activity}_{\text{Cerebellum}}}$$

Individual uptake ratio index was calculated not only for the static scanned 11 subjects but also for the dynamic scanned five subjects using the data obtained from an equivalent time-frame.

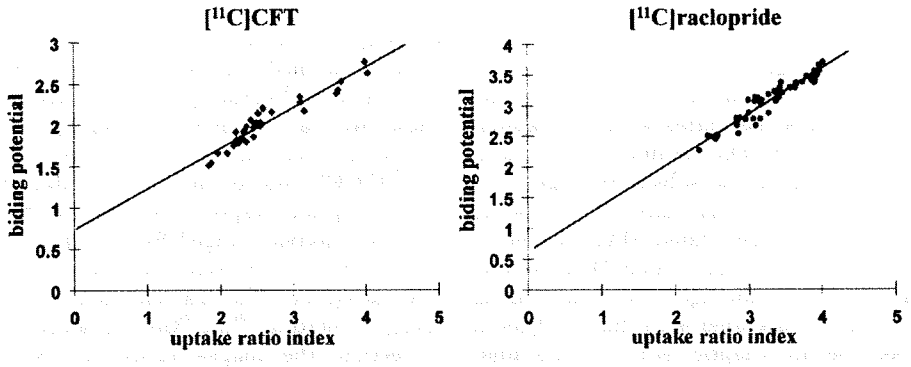

Fig. 1. Correlations between the binding potentials and uptake ratio indexes for [^{11}C]CFT (left) and [^{11}C]raclopride (right) in the striatum. Solid lines represent the regression lines. Linear correlation was significant for [^{11}C]CFT ($r = 0.95$; $P < 0.001$) and [^{11}C]raclopride ($r = 0.95$; $P < 0.001$).

Uptake ratio index and binding potential

To validate adopting the uptake ratio index, we examined the correlation between the binding potential (BP) and the uptake ratio index. Six ROIs were placed on the striatum of each dynamic scanned subject. The BP of each ROI for each tracer was estimated by a simplified reference region model using the cerebellum as a reference (Gunn et al., 1997). The cerebellum was selected as a reference region in the analysis, because it contains negligible levels of DATs, and D_2Rs. The uptake ratio index of each ROI was also estimated, as described earlier. Then, we compared the BPs of total 30 ROIs with the uptake ratio indexes of those.

Image processing of age-related decline on a voxel-by-voxel basis

To acquire the voxel-by-voxel regression images representing the slope of decline, we used SPM2 for the anatomical standardization and coregistration of the image. Individual [^{11}C]CFT and [^{11}C]raclopride uptake index images normalized to cerebellar activity, as described earlier, and MRI images were coregistered. Then, individual [^{11}C]CFT uptake index images were anatomically transformed into standard brain images using the in-house-developed [^{11}C]CFT image template, which was built in accordance with the strategy descried elsewhere (Meyer et al., 1999). The same transformation parameters were applied to the individual coregistered [^{11}C]raclopride uptake index images and MRI images. Additionally, we obtained the average MRI image from the transformed MRI images of 16 subjects.

To evaluate visually and statistically the regional differences in the aging effect within the striatum, we developed a software that could perform a linear regression analysis on a voxel-by-voxel basis between the age and uptake ratio index of [^{11}C]CFT and [^{11}C]raclopride. We also created parametric images mapping the slope of the regression line and the correlation coefficient (r) for each tracer. We called the former images age-related slope-of-decline images. We clipped the voxels with significant decline ($P < 0.01$) from the new images and superimposed them on the average MRI of 16 subjects.

Statistics

ROI-based analyses were performed by using the average of the right and the left uptake ratio indexes because of the following reasons. First, for each subregion of each tracer, neither the two-tailed paired t-test with Bonferroni correction nor analysis of variance with Levene's test revealed significant correlation between the right and the left uptake ratio indexes. Second, for each subregion of each tracer, the left-right difference in regression slope between the age and uptake ratio indexes was not statistically significant by using analysis of covariance. All statistical analyses were performed by using the software package JMP version 5.1.1 (SAS Institute, Cary, NC). P values less than 0.01 were considered to be statistically significant.

RESULTS

There were significant positive liner correlations between the BP and the uptake ratio index for both [^{11}C]CFT ($r = 0.95$; $P < 0.001$) and [^{11}C]raclopride ($r = 0.95$; $P < 0.001$), as shown in Figure 1. Therefore, we adopted the uptake ratio index for the further analysis.

ROI-based regression analysis revealed a highly significant age-related linear decline in the uptake ratio index of [^{11}C]CFT in the caudate nucleus ($r = 0.84$; $P < 0.001$), anterior putamen ($r = 0.75$; $P < 0.001$), and posterior putamen ($r = 0.79$; $P < 0.001$), and in that of [^{11}C]raclopride in the caudate nucleus ($r = 0.81$; $P < 0.001$), anterior putamen ($r = 0.80$;

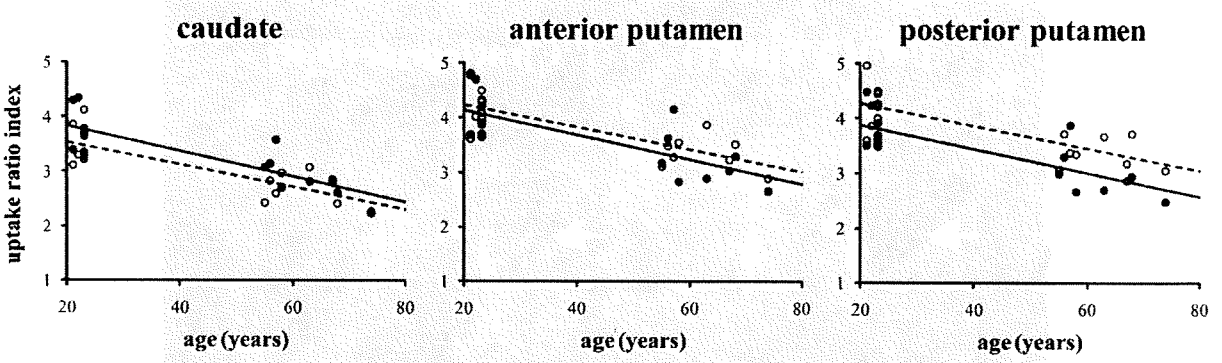

Fig. 2. Correlations between the age and uptake ratio indexes for [^{11}C]CFT (filled circles) and [^{11}C]raclopride (open circles) in the caudate (left), anterior putamen (middle), and posterior putamen (right). Solid lines represent the regression lines for [^{11}C]CFT and dotted lines, those for [^{11}C]raclopride. Linear correlation was significant for [^{11}C]CFT in the caudate (r = 0.84; P < 0.001), anterior putamen (r = 0.75; P < 0.001), and posterior putamen (r = 0.79; P < 0.001), and for [^{11}C]raclopride in the caudate nucleus (r = 0.81; P < 0.001), anterior putamen (r = 0.80; P < 0.001), and posterior putamen (r = 0.77; P < 0.001).

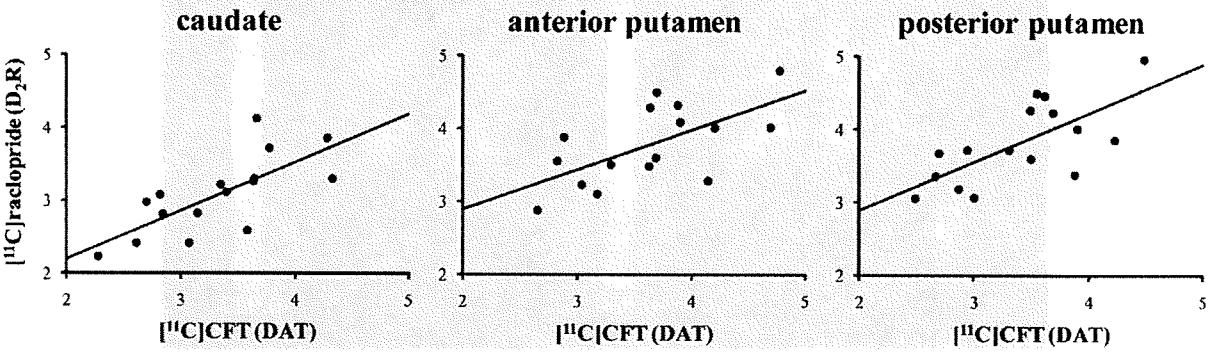

Fig. 3. Correlations between the uptake ratio indexes for [^{11}C]CFT and [^{11}C]raclopride in the caudate (left), anterior putamen (middle), and posterior putamen (right). Solid lines represent the regression lines. Linear correlation was significant for the caudate (r = 0.73; P = 0.001), anterior putamen (r = 0.64; P = 0.008), and posterior putamen (r = 0.70; P = 0.003).

P < 0.001), and posterior putamen (r = 0.77; P < 0.001), as shown in Figure 2. This decline corresponded to 6.1, 5.5, and 5.6% reduction per decade for [^{11}C]CFT uptake in the caudate nucleus, anterior putamen, and posterior putamen, respectively, and 5.8, 4.9, and 4.8% reduction per decade for [^{11}C]raclopride uptake in the caudate nucleus, anterior putamen, and posterior putamen. The [^{11}C]raclopride uptake was significantly correlated with the [^{11}C]CFT uptake in the caudate nucleus (r = 0.73; P = 0.001), anterior putamen (r = 0.64; P = 0.008), and posterior putamen (r = 0.70; P = 0.003), irrespective of age (Fig. 3).

For both [^{11}C]CFT and [^{11}C]raclopride, the age-related slope-of-decline images in Figure 4 showed that the significant decline was almost comparable to the results of ROI-based analysis, and we confirmed that most voxels in the striatum were included in the images. The decline rates in the caudate nucleus tended to be slightly higher than those in the subdivisions of the putamen. The difference between the decline rates in the anterior and posterior putamen was not obvious in both images. Moreover, two age-related slope-of-decline images were almost the same. Briefly, voxels with a high slope of decline in the age-related slope-of-decline image for [^{11}C]CFT also had a high slope of decline in the images for [^{11}C]raclopride. On the other hand, voxels with a low slope of decline in the images for [^{11}C]CFT also had a low slope of decline in the images for [^{11}C]raclopride. And although in ROI-based analysis there was no left-right statistically significant difference, in the image (shown in Finger 4) the decline rates in the left side tended to be higher than those in the right side in the striatum.

DISCUSSION

In this study, we simultaneously investigated the age-related change in DAT density and D_2R density, by particularly focusing on the regional difference. In addition to a conventional ROI-based analysis, in

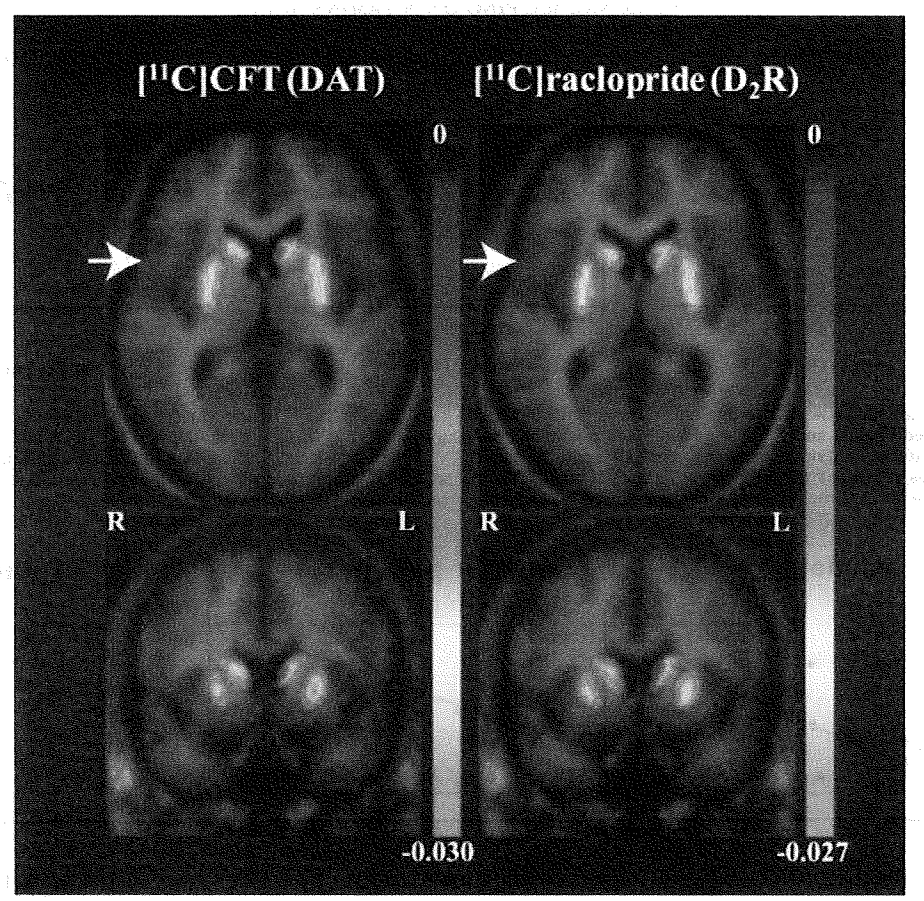

Fig. 4. The age-related slope-of-decline images superimposed on MRI for [^{11}C]CFT (left) and [^{11}C]raclopride (right) in transversal planes (top) at the level of the basal ganglia, and coronal planes (bottom) at the level of the white arrows marked in transversal planes. Voxels with significant decline ($P < 0.01$) were superimposed on MRI images. The degree of color scale represents the slope of the regression line between the age and uptake ratio index of each tracer on a voxel-by-voxel basis in the striatum and the scale value of −0.010 is equivalent to 2.6% reduction per decade. The images show the age-related regional rate of decline.

which the striatum was divided into three regions, we developed a novel method to create images mapping the slope of decline on a voxel-by-voxel basis so that we could investigate in detail the regional difference within the striatum in the aging effect on the nigrostriatal dopaminergic system. These images are equivalent to those made by visualizing the slope of the regression line between the age and uptake ratio index obtained by placing ROIs on every voxel. This new imaging technique superimposed on MRI can provide anatomical information in detail with high objectivity. This technique also completely eliminates arbitrariness and subjective elements, both of which are disadvantages of conventional ROI-based analysis. By reconfirming the result of the ROI-based analysis with the new imaging technique, the reliability of the research greatly improved. A possible limitation of this method is that the caudate nucleus could be influenced by the individual size of the lateral ventricles in the process of spatial normalization performed by SPM methods (Reig et al., 2007). Therefore, the caudate nucleus adjacent to the ventricles should be assessed carefully. Also, we should consider that the edge of the actual structure is susceptible to partial volume effects derived from original PET images.

In the process of creating the new imaging, the main problem was which template we should use for spatial normalization, because the use of different normalization strategies may alter noticeably the SPM map (Gispert et al., 2003). Two approaches to spatial normalization were considered. First was the ligand template approach, which was used in this study. Second was the MRI template approach: the coregistered MRI images to the PET images were spatially normalized to the SPM MRI template and the same transformations were applied to the PET images. On the basis of the study by Meyer et al.

TABLE I. In vivo human data: Age-related changes of dopamine transporter (DAT) and dopamine D_2-like receptor (D_2R)

In vivo	Name	Year	Type	Ligand	*n*	Age range (years)	Decreasing rate (% per decade)	Site
DAT	van Dyck et al.	1994	SPECT	[^{123}I]βCIT	28	18–83	8.0	Striatum
	Volkow et al.	1994	PET	[^{11}C]Cocaine	26	21–63	7.0	Striatum
	Ishikawa et al.	1996	SPECT	[^{123}I]βCIT-FP	15	45.5 ± 22.1[a]	3.3	Striatum
							6.4	Putamen
	Volkow et al.	1996a	PET	[^{11}C]d-Threo-methyphenidate	23	20–74	6.6	Striatum
	Kazumta et al.	1998	PET	[^{18}F]FPCIT	7	23–73	7.7	Caudate
							6.4	Putamen
	Rinne et al.	1998	PET	[^{11}C]βCFT	9	23–70	4.7	Caudate
							4.4	Putamen
	Volkow et al.	1998	PET	[^{11}C]d-Threo-methyphenidate	21	24–86	5[b]	Striatum
	Pirker et al.	2000	SPECT	[^{123}I]βCIT	16	21–75	6.6	Striatum
	Present data	2008	PET	[^{11}C]CFT	16	21–74	6.1	Caudate
							5.5	Anterior putamen
							5.6	Posterior putamen
D_2R	Wong et al.	1988	PET	[^{11}C]NMSP	36	19–71	8.3	Caudate
	Rinne et al.	1993	PET	[^{11}C]Raclopride	21	20–81	4.6	Striatum
	Volkow et al.	1996b	PET	[^{11}C]Raclopride	24	24–73	7.9	Striatum
	Wong et al.	1997	PET	[^{11}C]NMSP	24	13–79	8.4	Caudate
	Pohjlinen et al.	1998	PET	[^{11}C]Raclopride	54	19–82	5.0	Right striatum
							4.0	Left striatum
	Volkow et al.	1998	PET	[^{11}C]Raclopride	21	24–86	5[b]	Striatum
	Present data	2008	PET	[^{11}C]Raclopride	16	21–74	5.8	Caudate
							4.9	Anterior putamen
							4.8	Posterior putamen

[a]Mean ± SD.
[b]Estimated by us with the chart in original article.

TABLE II. In vitro post-mortem human data: Age-related changes of dopamine transporter (DAT) and dopamine D_2-like receptor (D_2R)

In vitro	Name	Year	Ligand	*n*	Age range (years)	Decreasing rate (% per decade)	Site
DAT	Zelnik et al.	1986	[^{3}H]GBR-12935	13	0–82	9[a]	Caudate
	Allard et al.	1989	[^{3}H]GBR-12935	20	19–100	8.8	Putamen
	De Keyser et al.	1990	[^{3}H]GBR-12935	32	19–88	9[a]	Putamen
D_2R	Severson et al.	1982	[^{3}H]Spiroperon	44	2–94	2.5	Caudate
			[^{3}H]ADTN			7.5	Caudate
	Rinne et al.	1987	[^{3}H]Spiroperidol	78	4–93	6.3	Putamen
	Seeman et al.	1987	[^{3}H]Spiroperon	247	0–94	2.2	Striatum
	Rinne et al.	1990	[^{3}H]Spiroperidol	65	6–93	3.8	Caudate
						3.7	Putamen

[a]Estimated by us with the chart in original article.

(1999), in which they suggested that the ligand template method provides a more reliable approach for spatial normalization of PET ligand-receptor images than the MRI template method, we chose the [^{11}C]CFT ligand template approach.

On the basis of the findings obtained from ROI-based analysis and the new imaging technique, we verified our hypothesis. In the ROI-based analysis, DAT density measured by [^{11}C]CFT PET was lost at rates of 6.1, 5.5, and 5.6% per decade in the caudate nucleus, anterior putamen, and posterior putamen, respectively. The corresponding rates for D_2R density measured by [^{11}C]raclopride PET were 5.8, 4.9, and 4.8% per decade, respectively. These results were comparable to previous neuroimaging studies that have shown the linear decline in DAT density ranging from 3.3 to 8.0% per decade (Ishikawa et al., 1996; Kazumata et al., 1998; Pirker et al., 2000; Rinne et al., 1998; van Dyck et al., 1995; Volkow et al., 1994, 1996a, 1998) and in D_2R density ranging from 4.6 to 8.4% (Pohjalainen et al., 1998; Rinne et al., 1993; Volkow et al., 1996b, 1998; Wong et al., 1988, 1997), as shown Table I. Despite sampling and methodological differences, previous in vitro postmortem studies using ligand binding techniques have also shown a significant age-related decline in DAT density (Allard and Marcusson, 1989; De Keyser et al., 1990; Zelnik et al., 1986) and D_2R density (Rinne, 1987; Rinne et al., 1990; Seeman et al., 1987; Severson et al., 1982), as shown Table II. In this study, the decline rates for both DAT and D_2R densities in the caudate nucleus were slightly higher than those in the putamen, as in the previous studies (Kazumata et al., 1998; Rinne et al., 1990, 1998). Meanwhile, the

decline rates for both DATs and D_2Rs in the anterior and posterior putamen were approximately the same. By using the age-related slope-of-decline images, we could reaffirm these tendencies.

However, despite of no left-right statistically significant deference in ROI-based analysis, the left side tended to be higher rate than the right side in the age-related slope-of-decline images. This might be because we placed relatively-small ROIs on the striatum to minimize partial volume effects. Actually small regions which include voxel with higher decreasing rate might be investigated preferentially. But with the age-related slope-of-decline images we could recognize the tendency by viewing the striatum macroscopically. Asymmetries of human cerebral functions have been revealed by neuroanatomy and neuroimaging studies (Laakso et al., 2000; Larisch et al., 1998; Toga and Thompson, 2003; Volkow et al., 1996a). There is also evidence from an animal study and a human study that the dopamine receptor asymmetry decreases with age (Giardino, 1996; Vernaleken et al., 2007). They indicated that the loss of asymmetry during normal aging may cause the left-right difference in the decreasing rate.

It has been confirmed that with an increase in age, neuronal loss occurs at a rate of 4.7–6.0% per decade in the substantia nigra (Fearnley and Lees, 1991; Gibb and Lees, 1991). Interestingly, this rate is almost same as the decline rate in DATs. The regional pattern of cell loss in the substantia nigra under normal aging is likely to preferentially affect the heavily pigmented neurons that are situated in the dorsomedial part of the substantia nigra (Gibb and Lees, 1991), an area where neuronal cells project preferentially to the caudate nucleus (Szabo, 1980). Our result, that the decline rate of DATs in the caudate nucleus was the fastest within the striatum, agreed with previous pathological studies. These findings indicate that the neuronal loss in the substantia nigra is strongly related to a significant decline of DATs during normal aging, and this supports our hypothesis. In other words, a decrease in DATs is likely to preferentially reflect neuronal loss in the substantia nigra.

In terms of the association between DATs and D_2Rs, our ROI-based analysis has shown significant correlation, irrespective of age in all three regions of the striatum. These results are comparable to those reported by Volkow et al. (1998). They evaluated DAT and D_2R densities by PET using [^{11}C]methylphenidate and [^{11}C]raclopride, respectively. They showed that DAT and D_2R densities decreased with age and that the association between DATs and D_2Rs was independent of age. And they suggested that a common mechanism regulates the expression of receptors and transporters. Furthermore, with the age-related slope-of-decline images, we could understand that the tendency of gradient distribution of the decreasing rate of DATs is almost same as that of D_2Rs throughout the striatum, not only along with the antero-posterior direction, but also along the ventro-dorsal and medio-lateral directions. These findings also supported our hypothesis. In other words, our results, in addition to the results presented by Volkow et al. (1998), suggested that a decrease in D_2Rs is likely to preferentially reflect the functional change in presynaptic and postsynaptic neurons, rather than neuronal loss in the striatum.

But actually the uptake of [^{11}C]raclopride reflects the total amount of dopamine D_2-like receptors, which include dopamine D_2, D_3, and D_4 receptor. Dopamine D_2 receptor has two isoforms, D_2L and D_2S, by a mechanism of alternative splicing (Picetti et al., 1997). D_2L acts mainly at postsynaptic sites and D_2S serves presynaptic autoreceptor functions (L'Hirondel et al., 1998; Mercuri et al., 1997). Therefore, the uptake of [^{11}C]raclopride could reflect presynaptic function corresponding to D_2 autoreceptor to some degree. But D_2S is less abundant than D_2L in the striatum (Giros et al., 1989; Guivarc'h et al., 1995; Monsma et al., 1989) and numerous D_2R imaging studies for parkinsonian disorders have indicated no discrepancy in the assumption that D_2R imaging could show mainly postsynaptic function (Piccini and Whone, 2004; Thobois et al., 2004). Then, we considered that the uptake of [^{11}C]raclopride reflects mainly postsynaptic function.

Considering our results, we could speculate that the age-related neuronal loss in the substantia nigra may trigger the structural change of presynaptic neurons (loss of DATs) in the striatum and this change may result in the functional change of postsynaptic neurons (loss of D_2Rs) in the striatum. Of course, the structural change of presynaptic neurons should also provoke the functional change of presynaptic neurons.

These functional changes include several presynaptic processes such as neurotransmitter synthesis, storage, metabolism, release, and reuptake/uptake, and postsynaptic processes such as receptor functioning, metabolism, and interactions with other neuromodulators (Reeves et al., 2002; Stanford et al., 2001). Functional changes such as the decrease in DAT mRNA (Bannon and Whitty, 1997) and changes in D_2R posttranscriptional regulation in striatal neurons (Sakata et al., 1992) have been reported.

The numbers of neurons and D_2R-containing cells in striatum also decrease during normal aging (Han et al., 1989; Meng et al., 1999); however, there exist no detailed histological reports on the regional differences in the decreasing rate. Future histological studies evaluating detailed regional differences in age-related decline of the numbers of D_2R-containing cells in the striatum are required. Such studies will help

to clarify the existence or nonexistence of the association between D_2R decline and cell loss in the striatum with aging. If such an association does not exist, our hypothesis will be supported more strongly.

In conclusion, we confirmed age-related decline in the striatal DAT and D_2R densities in normal subjects by conventional ROI-based analysis and by using age-related slope-of-decline images. The decreasing rate of DAT density in the caudate nucleus was the fastest within the striatum. The finding suggests that neuronal cell loss in the substantia nigra may be associated with age-related DAT decline in the striatum. The consistent association of the regional change in the decreasing rate between DATs and D_2Rs clearly demonstrated that the age-related DAT decline is associated functionally with the age-related D_2R decline. For investigating detailed regional mechanisms, the age-related slope-of-decline images were very useful.

ACKNOWLEDGMENTS

The authors thank Kazunori Kawamura, PhD; Takashi Oda, PhD; Miyoko Ando, RN; and Hiroko Tsukinari, RN, for their technical assistance.

REFERENCES

Allard P, Marcusson JO. 1989. Age-correlated loss of dopamine uptake sites labeled with [^{3}H]GBR-12935 in human putamen. Neurobiol Aging 10:661–664.

Antonini A, Leenders KL, Reist H, Thomann R, Beer HF, Locher J. 1993. Effect of age on D2 dopamine receptors in normal human brain measured by positron emission tomography and 11C-raclopride. Arch Neurol 50:474–480.

Bannon MJ, Whitty CJ. 1997. Age-related and regional differences in dopamine transporter mRNA expression in human midbrain. Neurology 48:969–977.

De Keyser J, Ebinger G, Vauquelin G. 1990. Age-related changes in the human nigrostriatal dopaminergic system. Ann Neurol 27:157–161.

Fearnley JM, Lees AJ. 1991. Ageing and Parkinson's disease: Substantia nigra regional selectivity. Brain 114 (Part 5):2283–2301.

Frost JJ, Rosier AJ, Reich SG, Smith JS, Ehlers MD, Snyder SH, Ravert HT, Dannals RF. 1993. Positron emission tomographic imaging of the dopamine transporter with 11C-WIN 35,428 reveals marked declines in mild Parkinson's disease. Ann Neurol 34:423–431.

Fujiwara T, Watanuki S, Yamamoto S, Miyake M, Seo S, Itoh M, Ishii K, Orihara H, Fukuda H, Satoh T, Kitamura K, Tanaka K, Takahashi S. 1997. Performance evaluation of a large axial field-of-view PET scanner: SET-2400W. Ann Nucl Med 11:307–313.

Giardino L. 1996. Right-left asymmetry of D1- and D2-receptor density is lost in the basal ganglia of old rats. Brain Res 720:235–238.

Gibb WR, Lees AJ. 1991. Anatomy, pigmentation, ventral and dorsal subpopulations of the substantia nigra, and differential cell death in Parkinson's disease. J Neurol Neurosurg Psychiatry 54:388–396.

Giros B, Sokoloff P, Martres MP, Riou JF, Emorine LJ, Schwartz JC. 1989. Alternative splicing directs the expression of two D2 dopamine receptor isoforms. Nature 342:923–926.

Gispert JD, Pascau J, Reig S, Martinez-Lazaro R, Molina V, Garcia-Barreno P, Desco M. 2003. Influence of the normalization template on the outcome of statistical parametric mapping of PET scans. Neuroimage 19:601–612.

Guivarc'h D, Vernier P, Vincent JD. 1995. Sex steroid hormones change the differential distribution of the isoforms of the D2 dopamine receptor messenger RNA in the rat brain. Neuroscience 69:159–166.

Gunn RN, Lammertsma AA, Hume SP, Cunningham VJ. 1997. Parametric imaging of ligand-receptor binding in PET using a simplified reference region model. Neuroimage 6:279–287.

Han Z, Kuyatt BL, Kochman KA, DeSouza EB, Roth GS. 1989. Effect of aging on concentrations of D2-receptor-containing neurons in the rat striatum. Brain Res 498:299–307.

Ishikawa T, Dhawan V, Kazumata K, Chaly T, Mandel F, Neumeyer J, Margouleff C, Babchyck B, Zanzi I, Eidelberg D. 1996. Comparative nigrostriatal dopaminergic imaging with iodine-123-beta CIT-FP/SPECT and fluorine-18-FDOPA/PET. J Nucl Med 37:1760–1765.

Kawamura K, Oda K, Ishiwata K. 2003. Age-related changes of the [^{11}C]CFT binding to the striatal dopamine transporters in the Fischer 344 rats: a PET study. Ann Nucl Med 17:249–253.

Kazumata K, Dhawan V, Chaly T, Antonini A, Margouleff C, Belakhlef A, Neumeyer J, Eidelberg D. 1998. Dopamine transporter imaging with fluorine-18-FPCIT and PET. J Nucl Med 39:1521–1530.

L'Hirondel M, Cheramy A, Godeheu G, Artaud F, Saiardi A, Borrelli E, Glowinski J. 1998. Lack of autoreceptor-mediated inhibitory control of dopamine release in striatal synaptosomes of D2 receptor-deficient mice. Brain Res 792:253–262.

Laakso A, Vilkman H, Alakare B, Haaparanta M, Bergman J, Solin O, Peurasaari J, Rakkolainen V, Syvalahti E, Hietala J. 2000. Striatal dopamine transporter binding in neuroleptic-naive patients with schizophrenia studied with positron emission tomography. Am J Psychiatry 157:269–271.

Langer ONK, Dolle F, Lundkvist C, Sandell J, Swahn CG, Vaufrey F, Crouzel C, Maziere B, Halldin C. 1999. Precursor synthesis and radiolabelling of the dopamine D2 receptor ligand [^{11}C]raclopride from [^{11}C]methyl triflate. J Labelled Comp Radiopharm 42:1183–1193.

Larisch R, Meyer W, Klimke A, Kehren F, Vosberg H, Muller-Gartner HW. 1998. Left-right asymmetry of striatal dopamine D2 receptors. Nucl Med Commun 19:781–787.

Meng SZ, Ozawa Y, Itoh M, Takashima S. 1999. Developmental and age-related changes of dopamine transporter, and dopamine D1 and D2 receptors in human basal ganglia. Brain Res 843:136–144.

Mercuri NB, Saiardi A, Bonci A, Picetti R, Calabresi P, Bernardi G, Borrelli E. 1997. Loss of autoreceptor function in dopaminergic neurons from dopamine D2 receptor deficient mice. Neuroscience 79:323–327.

Meyer JH, Gunn RN, Myers R, Grasby PM. 1999. Assessment of spatial normalization of PET ligand images using ligand-specific templates. Neuroimage 9:545–553.

Monsma FJ Jr, McVittie LD, Gerfen CR, Mahan LC, Sibley DR. 1989. Multiple D2 dopamine receptors produced by alternative RNA splicing. Nature 342:926–929.

Piccini P, Whone A. 2004. Functional brain imaging in the differential diagnosis of Parkinson's disease. Lancet Neurol 3:284–290.

Picetti R, Saiardi A, Abdel Samad T, Bozzi Y, Baik JH, Borrelli E. 1997. Dopamine D2 receptors in signal transduction and behavior. Crit Rev Neurobiol 11:121–142.

Pirker W, Asenbaum S, Hauk M, Kandlhofer S, Tauscher J, Willeit M, Neumeister A, Praschak-Rieder N, Angelberger P, Brucke T. 2000. Imaging serotonin and dopamine transporters with 123I-beta-CIT SPECT: binding kinetics and effects of normal aging. J Nucl Med 41:36–44.

Pohjalainen T, Rinne JO, Nagren K, Syvalahti E, Hietala J. 1998. Sex differences in the striatal dopamine D2 receptor binding characteristics in vivo. Am J Psychiatry 155:768–773.

Reeves S, Bench C, Howard R. 2002. Ageing and the nigrostriatal dopaminergic system. Int J Geriatr Psychiatry 17:359–370.

Reig S, Penedo M, Gispert JD, Pascau J, Sanchez-Gonzalez J, Garcia-Barreno P, Desco M. 2007. Impact of ventricular enlargement on the measurement of metabolic activity in spatially normalized PET. Neuroimage 35:748–758.

Rinne JO. 1987. Muscarinic and dopaminergic receptors in the aging human brain. Brain Res 404:162–168.

Rinne JO, Hietala J, Ruotsalainen U, Sako E, Laihinen A, Nagren K, Lehikoinen P, Oikonen V, Syvalahti E. 1993. Decrease in human striatal dopamine D2 receptor density with age: A PET study with [^{11}C]raclopride. J Cereb Blood Flow Metab 13:310–314.

Rinne JO, Lonnberg P, Marjamaki P. 1990. Age-dependent decline in human brain dopamine D1 and D2 receptors. Brain Res 508:349–352.

Rinne JO, Sahlberg N, Ruottinen H, Nagren K, Lehikoinen P. 1998. Striatal uptake of the dopamine reuptake ligand [^{11}C]beta-CFT is reduced in Alzheimer's disease assessed by positron emission tomography. Neurology 50:152–156.

Sakata M, Farooqui SM, Prasad C. 1992. Post-transcriptional regulation of loss of rat striatal D2 dopamine receptor during aging. Brain Res 575:309–314.

Seeman P, Bzowej NH, Guan HC, Bergeron C, Becker LE, Reynolds GP, Bird ED, Riederer P, Jellinger K, Watanabe S, Tourtellotte WW. 1987. Human brain dopamine receptors in children and aging adults. Synapse 1:399–404.

Severson JA, Marcusson J, Winblad B, Finch CE. 1982. Age-correlated loss of dopaminergic binding sites in human basal ganglia. J Neurochem 39:1623–1631.

Stanford JA, Hebert MA, Gerhardt GA. 2001. Biochemical and anatomical changes in basal ganglia of aging animals.Hof PR, Mobbs cV, editors. San Diego: Academic Press. 727–736 p.

Stark AK, Pakkenberg B. 2004. Histological changes of the dopaminergic nigrostriatal system in aging. Cell Tissue Res 318:81–92.

Szabo J. 1980. Organization of the ascending striatal afferents in monkeys. J Comp Neurol 189:307–321.

Thobois S, Jahanshahi M, Pinto S, Frackowiak R, Limousin-Dowsey P. 2004. PET and SPECT functional imaging studies in Parkinsonian syndromes: From the lesion to its consequences. Neuroimage 23:1–16.

Toga AW, Thompson PM. 2003. Mapping brain asymmetry. Nat Rev Neurosci 4:37–48.

van Dyck CH, Seibyl JP, Malison RT, Laruelle M, Wallace E, Zoghbi SS, Zea-Ponce Y, Baldwin RM, Charney DS, Hoffer PB. 1995. Age-related decline in striatal dopamine transporter binding with iodine-123-beta-CITSPECT. J Nucl Med 36:1175–1181.

Vernaleken I, Weibrich C, Siessmeier T, Buchholz HG, Rosch F, Heinz A, Cumming P, Stoeter P, Bartenstein P, Grunder G. 2007. Asymmetry in dopamine D(2/3) receptors of caudate nucleus is lost with age. Neuroimage 34:870–878.

Volkow ND, Fowler JS, Wang GJ, Logan J, Schlyer D, MacGregor R, Hitzemann R, Wolf AP. 1994. Decreased dopamine transporters with age in health human subjects. Ann Neurol 36:237–239.

Volkow ND, Ding YS, Fowler JS, Wang GJ, Logan J, Gatley SJ, Hitzemann R, Smith G, Fields SD, Gur R. 1996a. Dopamine transporters decrease with age. J Nucl Med 37:554–559.

Volkow ND, Wang GJ, Fowler JS, Logan J, Gatley SJ, MacGregor RR, Schlyer DJ, Hitzemann R, Wolf AP. 1996b. Measuring age-related changes in dopamine D2 receptors with 11C-raclopride and 18F-N-methylspiroperidol. Psychiatry Res 67:11–16.

Volkow ND, Wang GJ, Fowler JS, Ding YS, Gur RC, Gatley J, Logan J, Moberg PJ, Hitzemann R, Smith G, Pappas N. 1998. Parallel loss of presynaptic and postsynaptic dopamine markers in normal aging. Ann Neurol 44:143–147.

Wong DF, Broussolle EP, Wand G, Villemagne V, Dannals RF, Links JM, Zacur HA, Harris J, Naidu S, Braestrup C, Wagner HN Jr, Gjedde A. 1988. In vivo measurement of dopamine receptors in human brain by positron emission tomography. Age and sex differences. Ann NY Acad Sci 515:203–214.

Wong DF, Yung B, Dannals RF, Shaya EK, Ravert HT, Chen CA, Chan B, Folio T, Scheffel U, Ricaurte GA, Neumeyer JL, Wagner HN Jr, Kuhar MJ. 1993. In vivo imaging of baboon and human dopamine transporters by positron emission tomography using [^{11}C]WIN 35,428. Synapse 15:130–142.

Wong DF, Young D, Wilson PD, Meltzer CC, Gjedde A. 1997. Quantification of neuroreceptors in the living human brain. III. D2-like dopamine receptors: Theory, validation, and changes during normal aging. J Cereb Blood Flow Metab 17:316–330.

Zelnik N, Angel I, Paul SM, Kleinman JE. 1986. Decreased density of human striatal dopamine uptake sites with age. Eur J Pharmacol 126:175–176.

Mapping of brain acetylcholinesterase alterations in Lewy body disease by PET

H. Shimada, MD
S. Hirano, MD, PhD
H. Shinotoh, MD, PhD
A. Aotsuka, MD, PhD
K. Sato, MD, PhD
N. Tanaka, MD, PhD
T. Ota, MD, PhD
M. Asahina, MD, PhD
K. Fukushi, PhD
S. Kuwabara, MD, PhD
T. Hattori, MD, PhD
T. Suhara, MD, PhD
T. Irie, PhD

Address correspondence and reprint requests to Dr. Hitoshi Shinotoh, Molecular Neuroimaging Group, Molecular Imaging Center, National Institute of Radiological Sciences, 4-9-1 Anagawa, Inage-ku, Chiba-shi, Chiba, 260-8555, Japan
BQV10131@nifty.ne.jp

ABSTRACT

Objective: To characterize brain cholinergic deficits in Parkinson disease (PD), PD with dementia (PDD), and dementia with Lewy bodies (DLB).

Methods: Participants included 18 patients with PD, 21 patients with PDD/DLB, and 26 healthy controls. The PD group consisted of nine patients with early PD, each with a disease duration of less than 3 years, five of whom were de novo PD patients, and nine patients with advanced PD, each with a disease duration greater than or equal to 3 years. The PDD/DLB group consisted of 10 patients with PDD and 11 patients with DLB. All subjects underwent PET scans with *N*-[^{11}C]-methyl-4-piperidyl acetate to measure brain acetylcholinesterase (AChE) activity. Brain AChE activity levels were estimated voxel-by-voxel in a three-compartment analysis using the arterial input function, and compared among our subject groups through both voxel-based analysis using the statistical parametric mapping software SPM5 and volume-of-interest analysis.

Results: Among patients with PD, AChE activity was significantly decreased in the cerebral cortex and especially in the medial occipital cortex (% reduction compared with the normal mean = −12%) (false discovery rate-corrected *p* value <0.01). Patients with PDD/DLB, however, had even lower AChE activity in the cerebral cortex (% reduction = −27%) ($p < 0.01$). There was no significant difference between early PD and advanced PD groups or between DLB and PDD groups in the amount by which regional AChE activity in the brain was reduced.

Conclusions: Brain cholinergic dysfunction occurs in the cerebral cortex, especially in the medial occipital cortex. It begins in early Parkinson disease, and is more widespread and profound in both Parkinson disease with dementia and dementia with Lewy bodies. ***Neurology***® **2009;73:273-278**

GLOSSARY

AChE = acetylcholinesterase; **ANOVA** = analysis of variance; **BA** = Brodmann area; **DLB** = dementia with Lewy bodies; ***DSM-IV*** = *Diagnostic and Statistical Manual of Mental Disorders*, 4th edition; **FDR** = false discovery rate; **FWE** = family-wise error; **HC** = healthy controls; **LBD** = Lewy body disease; **MMSE** = Mini-Mental State Examination; **MNI** = Montreal Neurological Institute; **PD** = Parkinson disease; **PDD** = Parkinson disease with dementia; **VOI** = volume of interest.

Parkinson disease (PD) is frequently associated with cognitive deficits which can range from subtle deficiencies to dementia.[1] These cognitive deficits are attributed mainly to Lewy body pathology in the cerebral cortex and limbic structures, but also partly to Alzheimer disease (AD)-type pathology and to nigral and brainstem pathology associated with PD.[1] Alterations of dopaminergic, serotonergic, and noradrenergic systems may also underlie the cognitive disturbances that are seen in PD,[2,3] along with alterations of ascending cholinergic systems from the basal forebrain and the brainstem, which have been implicated as pivotal players in cognitive function and especially in attention and consciousness.[4-6] Loss of cholinergic neurons in the nucleus basalis of Mynert has been observed in postmortem PD brains, and has been thought to contribute to cognitive decline in PD.[7]

Dementia with Lewy bodies (DLB) is the second most frequent neurodegenerative dementia, after AD. DLB is diagnosed when dementia occurs before or concurrently with parkinsonism, while

Supplemental data at www.neurology.org

Editorial, page 256

e-Pub ahead of print on May 27, 2009, at www.neurology.org.
From the Department of Neurology (H. Shimada, A.A., M.A., S.K., and T.H.), Graduate School of Medicine, Chiba University; and the Molecular Imaging Center (H.S., H. Shinotoh, K.S., N.T., T.O., K.F., T.S., T.I.), National Institute of Radiological Sciences, Chiba, Japan.
Dr. Asahina is funded by a Grant-in-Aid for Scientific Research (17590861).

Disclosure: The authors report no disclosures.

Table 1 **Clinical profiles of patients with Parkinson disease (PD), PD with dementia (PDD), and dementia with Lewy bodies (DLB)**

	Healthy controls	PD		PDD/DLB	
		Early PD	Advanced PD	PDD	DLB
No. of subjects	26		18		21
Male:female	14:12	6:3	4:5	4:6	6:5
Age, y	63.8 ± 10.1	65.4 ± 10.7	68.8 ± 6.2	75.0 ± 5.3	77.7 ± 5.9
Disease duration, y	—	1.8 ± 0.5	6.7 ± 3.4	9.4 ± 2.8	3.7 ± 2.7
Hoehn & Yahr stage		2.3 ± 0.7	2.9 ± 0.9	3.8 ± 1.0	3.8 ± 1.1
Levodopa equivalents, mg	—	98 ± 149	425 ±200	339 ± 108	95 ± 123
MMSE	29.4 ± 1.0	27.6 ± 2.1	27.7 ± 2.3	18.0 ± 5.6	17.8 ± 5.3

Values are mean ± SD.
The PD group consists of early stage PD (early PD: disease duration <3 years) and advanced stage PD (advanced PD: disease duration ≥3 years).
MMSE = Mini-Mental State Examination.

PD with dementia (PDD) is diagnosed when dementia occurs in the context of well-established PD.[8] PD and DLB are regarded as two ends of a spectrum of Lewy body disease (LBD). Cholinergic systems also may play a role in these diseases: widespread and profound reduction of choline acetyltransferase activity has been observed in postmortem brains with DLB.[9,10]

Brain cholinergic function can be estimated by measuring acetylcholinesterase (AChE) activity in the brain with PET and the radiolabeled acetylcholine analogues *N*-[^{11}C]-methyl-4-piperidyl acetate (MP4A)[11] and *N*-[^{11}C]-methyl-4-piperidyl propionate (MP4P).[12] Previous PET studies showed a significant reduction in cortical AChE activity in PD,[13-15] and a more sizeable decrease in cortical AChE activity in PDD and DLB than in AD.[14] It is not well known, however, when brain cholinergic deficits occur or how they develop in PD. Furthermore, the possibility of a difference in brain cholinergic deficits between PDD and DLB has not been explored in detail.

To elucidate these questions, we used PET to investigate alterations in brain AChE activity in early PD, advanced PD, PDD, and DLB.

METHODS

Subjects. Participants were 18 patients with PD, 21 patients with PDD/DLB, and 26 healthy controls (HC; table 1). The PD group consisted of nine patients with early PD, each with a disease duration of less than 3 years, five of whom were de novo PD patients, and nine patients with advanced PD, each with a disease duration greater than or equal to 3 years. The patients with PD were also divided into six subjects with age at onset less than 60 years and 12 subjects with age at onset older than 60 years to determine whether patients with younger onset PD have less cholinergic denervation compared to the patients with older onset PD. The PDD/DLB group consisted of 10 patients with PDD and 11 patients with DLB. The patients with DLB were also divided into six younger subjects with age less than 78.2 years (median age of all DLB subjects) (73.9 ± 4.7 years) and five subjects with age older than 78.2 years (82.4 ± 3.4 years), and HC subjects were divided into 13 younger subjects with age less than 63.7 years (median age of all HC subjects) (56.3 ± 6.1 years) and 13 older subjects with age older than 63.7 years (71.2 ± 7.3 years) to confirm whether there are age effects. HC had no history of neurologic disorders and no abnormalities assessed in a general physical and neurologic examination. Diagnoses of PD were made according to the diagnostic criteria of the UK Brain Bank[16]; DLB diagnoses were made according to the DLB Consortium criteria.[8] In subjects with PDD, dementia was diagnosed according to the criteria found in the *DSM-IV*.[17] PDD and DLB could be distinguished from one another if at least 1 year had passed between the onset of dementia and that of parkinsonism, or vice versa.[8]

Levodopa equivalents were estimated as follows: 100 mg of levodopa with a dopa-decarboxylase inhibitor (Menesit®, Banyu Pharmaceutical Co., Ltd., Tokyo, Japan; EC-dopal®, Kyowa Hakko Kirin Co., Ltd., Tokyo, Japan) = 1 mg of pergolide (Permax®, Eli Lilly Japan K.K., Hyogo, Japan) = 1.5 mg of cabergoline (Cabaser®, Pfizer Japan Inc., Tokyo, Japan) = 10 mg of bromocriptine (Parodel®, NOVARTIS Pharma K.K., Tokyo, Japan) = 1 mg of pramipexole (Bi-Sifrol®, Nippon Boehringer Ingelheim Co., Ltd., Tokyo, Japan).[18,19] None of the patients was treated with anticholinergic agents or choline esterase inhibitors. Medications were discontinued at least 15 hours before each PET scan. All patients were assessed using the Unified Parkinson's Disease Rating Scale and the Mini-Mental State Examination (MMSE).[20] HC subjects were cognitively unimpaired and free from medications having central nervous action. The PET study was approved by the Institutional Review Board of the National Institute of Radiologic Sciences. Written informed consent was obtained from all subjects or from their spouses or other close family members.

PET scan. PET images were acquired with an ECAT Exact-47 scanner or an HR+ scanner (CTI PET Systems, Inc., Knoxville, TN). We scanned two HC subjects using the two types of PET scanner and directly compared the results to confirm that the choice of PET scanner made no difference in our results on a voxel level (false discovery rate [FDR]-cluster-corrected p value >0.05). Subjects were examined with their eyes closed and their ears unplugged in a quiet room; their heads were restrained with a band extending across the forehead attached to the headrest. An examiner carefully monitored head movement during each scan with laser beams, and corrected the head position if the subject moved. A dose (about 740 MBq) of [^{11}C]MP4A was IV injected for 60 seconds, and sequential PET scans were performed for 40 minutes with arterial blood sampling.[11]

All imaging data were preprocessed and analyzed with statistical parametric mapping software (SPM5; http://www.fil.ion.ucl.ac.uk/spm), operating in the Matlab software environment (version 7.4; MathWorks, Natick, MA). Each PET image was normalized to a novel [^{11}C]MP4A PET template, which we created using PET and MRI from 11 HC subjects according to the standard method.[21] Briefly, T1-weighted MRI scans were coreg-

Figure 1 Cortical k_3 declines in each group compared with healthy controls

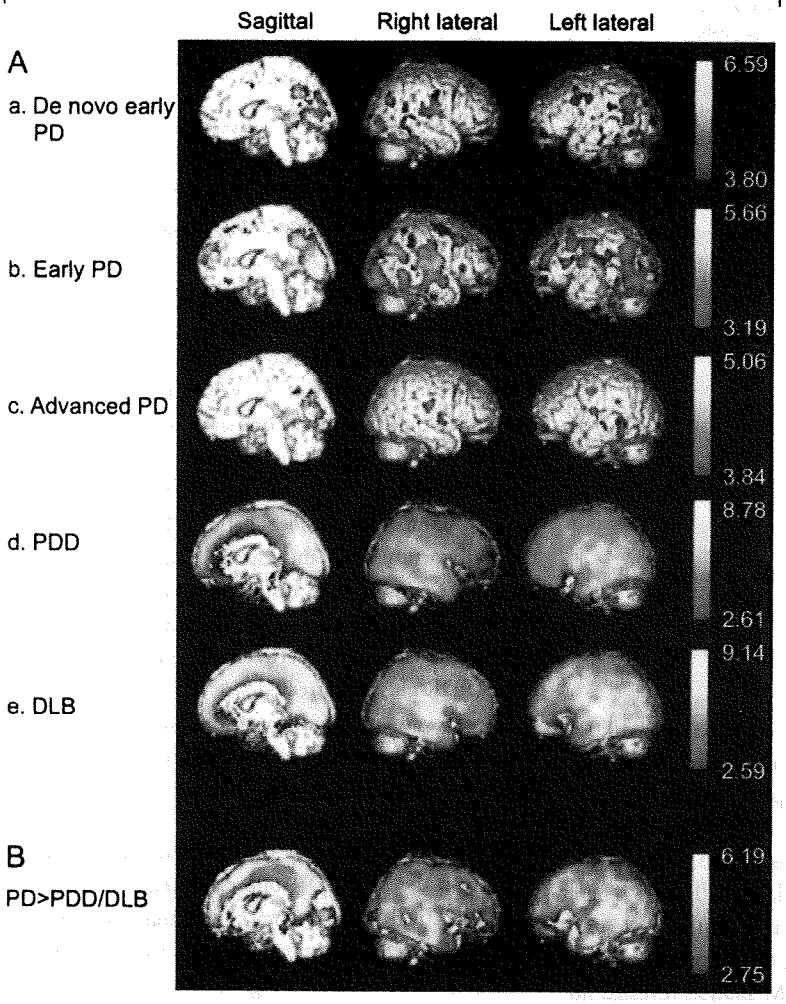

(A) Regions where a reduction in k_3 (acetylcholinesterase activity) was observed in de novo Parkinson disease (PD) (n = 5), early stage PD (n = 9), advanced stage PD (n = 9), Parkinson disease with dementia (PDD) (n = 10), and dementia with Lewy bodies (DLB) (n = 11), compared with healthy controls (FDR-corrected $p < 0.01$, $k > 26$, age as a covariate). (B) Regions where a greater reduction in k_3 was observed in the PDD/DLB group than in the PD group (FDR-corrected $p < 0.01$, $k > 26$, age as a covariate). The red-to-yellow color gradient indicates the locations of the voxels with reduced k_3 values and the amount by which these values were reduced. Note that the color bars indicating t score are different among the different analyses.

istered to the PET integral images, and the spatial normalization of the MR images to the SPM2 T1 MRI template was applied to the integral images. These integral images were averaged and smoothed with an isotropic 8-mm Gaussian kernel to form our [^{11}C]MP4A template.

PET images were smoothed with an isotropic 12-mm Gaussian kernel after normalization. Then we estimated K_1 value, an index of blood flow, and k_3 value, an index of AChE activity, for each image with a nonlinear least square analysis in a three-compartment model using the metabolite corrected arterial input function.[11] We used custom software designed by IDL (version 6.0; Jicoux Datasystems, Inc., Tokyo, Japan) to calculate a voxel-based K_1 value and k_3 value from each image. Voxel-based analysis of K_1 values and k_3 values among groups was performed using SPM5 with age as a covariate. The k_3 values were also compared between younger onset and older onset PD groups, and between younger DLB and older DLB groups by both voxel-based analysis and volume-of-interest analysis. We proceeded with statistical analyses when the FDR-cluster-corrected p value was less than 0.01. All results were expressed in the Montreal Neurological Institute coordinate space.

Volumes of interest (VOIs) were identified on k_3 images in each subject's frontal lobe, temporal lobe, parietal lobe, occipital lobe, hippocampus, amygdala, and Brodmann areas (BAs), using the Wake Forest University Pick Atlas (http://fmri.wfubmc.edu/cms/software).

Cortical k_3 values were calculated for each subject as the mean of the k_3 values for that subject's frontal, temporal, parietal, and occipital cortices in both hemispheres. The correlation between cortical k_3 values and MMSE scores, and that between cortical k_3 values and disease duration, and that between cortical k_3 values and voxel-by-voxel K_1 values with age as a covariate were analyzed in LBD patients.

RESULTS There was no significant difference in gender ratios among the HC, PD, PDD, and DLB groups. Both patients with DLB and patients with PDD were older than HC subjects [$F(4,64) = 7.0$, $p < 0.05$, one-way analysis of variance (ANOVA)], and patients with DLB were older than patients with early PD [$F(4,64) = 7.0$, $p < 0.05$, one-way ANOVA]. Patients with PDD/DLB were older than both HC subjects and patients with PD [$F(2,64) = 13.5$, $p < 0.01$, one-way ANOVA]. Older DLB subjects were older than younger DLB subjects (unpaired t test, $p < 0.01$). There was no significant difference in age or gender ratios among the older HC, de novo early PD, early PD, advanced PD, PDD, and younger DLB groups. There was no difference in disease duration between the PD and PDD/DLB groups ($p = 0.10$, unpaired t test). MMSE scores in the PDD/DLB group were lower than those in the HC and PD groups [$F(2,64) = 78.8$, $p < 0.01$, one-way ANOVA].

SPM analysis showed clusters of voxels with reduced k_3 values in the cerebral cortices of de novo early PD, early PD, and advanced PD patients, compared with those seen in HC subjects (FDR-cluster-corrected $p < 0.01$; figure 1A, a, b, c; table 2). The most significant reduction in cerebral cortical k_3 was detected in BA 18, in the de novo early PD (table 2), early PD ([28, −82, −4], $Z_{max} = 5.04$, family-wise error [FWE]-corrected $p < 0.01$), and advanced PD groups ([12, −70, 4], $Z_{max} = 4.60$, FWE-corrected $p < 0.01$). SPM analysis between the early PD and advanced PD groups revealed no cluster with different k_3 values (FDR-cluster-corrected $p > 0.01$). There was not any significant difference in brain AChE activity between patients with younger onset PD and patients with older onset PD (FDR-cluster-corrected $p > 0.05$).

The k_3 values in the PDD and DLB groups were reduced compared to those in the HC group in almost all cortical areas and especially in the posterior

Table 2 **Regions with significant reduction in cortical MP4A k_3 in the de novo early Parkinson disease group compared with the healthy controls group (de novo early Parkinson disease < healthy control)**

Regions	Z_{max}	Coordinates (MNI) x	y	z	Voxels per cluster
R middle occipital gyrus (BA18)	5.08*	28	−80	0	2,478
L cuneus (BA19)	4.47	−22	−78	30	
L superior temporal gyrus (BA39)	4.97	−44	−52	30	864
R precuneus (BA7)	4.91	26	−60	32	625
R posterior cingulate (BA30)	3.59	24	−56	18	
R precentral gyrus (BA6)	4.42	50	−14	28	661
Medial frontal gyrus (BA32)	4.38	−6	8	44	203
R middle temporal gyrus (BA22)	3.73	48	−40	6	224
R inferior temporal gyrus (BA37)	3.71	54	−52	−2	
L fusiform gyrus (BA37)	4.23	−44	−62	−10	229
L precentral gyrus (BA4)	4.05	−58	−8	34	319

Coordinates at which a significant reduction in k_3 was observed in the de novo early Parkinson disease group compared with the HC group (FDR-corrected $p < 0.01, k > 26$).
*Family-wise error-corrected $p < 0.005, k > 26$.
MNI = Montreal Neurological Institute; BA = Brodmann area; FDR = false discovery rate.

cortical regions (FDR-cluster-corrected $p < 0.01$, figure 1A, d, e). The most significant reduction was observed in the left lateral temporal lobe in the PDD ([−56, −46, −12], $Z_{max} = 6.99$, FWE-corrected $p < 0.001$) and DLB groups ([−56, −24, −2], $Z_{max} = 7.18$, FWE-corrected, $p < 0.001$). There was no significant reduction in k_3 values in the medial temporal cortex including the hippocampus and amygdala (figure 1A, d, e). SPM analysis revealed no cluster with altered k_3 values between the PDD and DLB groups (FDR-cluster-corrected $p > 0.01$), although the decline in cortical k_3 values tended to be greater in the DLB group (% reduction compared with the normal mean = −27.1%) than in the PDD group (−23.4%).

Cortical k_3 values were lower in both the PD group (−11.8%) and the PDD/DLB group (−26.8%) than in the HC group [$F(2,64) = 44.7$, $p < 0.01$, one-way ANOVA]. When the PDD/DLB and PD groups were compared, SPM analysis showed a reduction of k_3 values in the inferior temporal gyrus (BA20), the supramarginal gyrus (BA40) (FWE-corrected $p < 0.005$), and the posterior cingulate gyrus (BA31) (FWE-corrected $p < 0.01$) in the PDD/DLB group, compared with the equivalent values in the PD group (figure 1B, table 3).

There was not any significant difference in brain AChE activity between younger patients with DLB (% reduction compared with the age-matched older normal mean = −28.5%) and older patients with DLB (−28.9%) (FDR-cluster-corrected $p > 0.05$). Results of SPM analysis among older HC, de novo early PD, early PD, advanced PD, PDD, and younger DLB groups did not differ from those among HC, de novo early PD, advanced PD, PDD, and DLB groups (figure e-1 on the *Neurology*® Web site at www.neurology.org).

There was a correlation between cortical k_3 values and MMSE scores in patients with PD and patients with PDD/DLB ($r = 0.47$, $p < 0.01$, figure 2B). VOI analysis revealed that the strongest correlation between k_3 values and MMSE scores occurred in the posterior cingulate gyrus (BA31) in patients with LBD ($r = 0.57, p < 0.0005$).

SPM analysis did not show a cluster of voxels with a significant reduction of K_1 values in the cerebral cortices of the PD group compared with those seen in HC subjects (FDR-cluster-corrected $p > 0.05$). The K_1 values in the PDD and DLB groups were reduced compared to those in the HC group in almost all cortical areas and especially in the occipital cortical regions (FDR-cluster-corrected $p < 0.05$) (figure e-2). There was no significant voxel with a significant correlation between K_1 and cortical k_3 value (FDR-cluster-corrected $p > 0.01$).

There were no significant correlations between cortical k_3 values and disease duration or age ($p > 0.21$).

DISCUSSION Our study revealed four major findings. First, the early PD group exhibited a reduction in AChE activity in the cerebral cortex, and especially in the medial occipital cortex (BA 18). Even de novo early PD cases exhibited significant reductions in AChE activity in the medial occipital cortex (BA 18), suggesting that brain cholinergic dysfunction occurs at a very early stage of PD and may precede the manifestation of motor symptoms in PD. The ascending cholinergic system from the basal forebrain may play a role in the modulation of postsynaptic visual processing.[22] A SPECT study demonstrated that occipital hypoperfusion is associated with impairment of visual perception in PD.[23] We did not, however, note any significant reduction of K_1 values in the occipital cortex in patients with PD nor any significant correlation between K_1 and cortical k_3 in any brain region in patients with LBD, suggesting independent changes of cerebral blood flow and AChE activity in patients with LBD.

The second major finding of our study is that there is no significant difference in brain AChE activity levels between patients with early PD and patients with advanced PD. This observation suggests that cholinergic deficits do not progress during the course of PD without dementia, even at advanced stages. Our results may suggest that cholinergic denervation does not parallel the degree of dopaminergic dener-

Table 3 **Regions with significant reduction in cortical MP4A k_3 in the PDD group compared with the PD group (PDD/DLB < PD)**

Regions	Z_{max}	Coordinates (MNI) x	y	z	Voxels per cluster
L inferior temporal gyrus (BA20)	5.40*	−54	−46	−12	72,546
L supramarginal gyrus (BA40)	5.30*	−50	−50	18	
Posterior cingulate (BA31)	5.09	−2	−38	40	

Coordinates at which a significant reduction in k_3 was observed in the PDD/DLB group compared with the PD group (FDR-corrected $p < 0.01$, $k > 26$).
*Family-wise error-corrected $p < 0.005$, $k > 26$.
PDD = Parkinson disease with dementia; DLB = dementia with Lewy bodies; PD = Parkinson disease; MNI = Montreal Neurological Institute; BA = Brodmann area; FDR = false discovery rate.

vation. Hilker and colleagues[15] investigated possible interdependence of dopaminergic and cholinergic transmitter dysfunction in PD and PDD. The cortical k_3 in [^{11}C]MP4A PET and striatal [^{18}F]fluorodopa uptake did not correlate with each other in the patients, although the authors found a cluster with significant covariance of striatal [^{18}F]fluorodopa uptake and cortical k_3 reduction in the middle frontal gyrus in PD and several clusters in frontal and temporo-parietal cortices in PDD. The striatal [^{18}F]fluorodopa uptake was significantly decreased in PD and PDD without significant differences between the groups in their study. Therefore, our result in PD is compatible with their result in PD. Interestingly, according to our SPM analysis, there was a tendency that AChE activity in the cerebral cortex was decreased more in the early PD group than the advanced PD group, suggesting that the early PD group might consist of some patients with PD who will eventually develop PDD and others who will develop advanced PD without dementia. The average disease duration in the advanced PD group was 6.7 years yet the average Hoehn and Yahr stage was 2.9. Taken together, the advanced PD group might be a benign PD subtype in the present study.

Figure 2 **Correlation between Mini-Mental State Examination (MMSE) scores and cortical k_3 values**

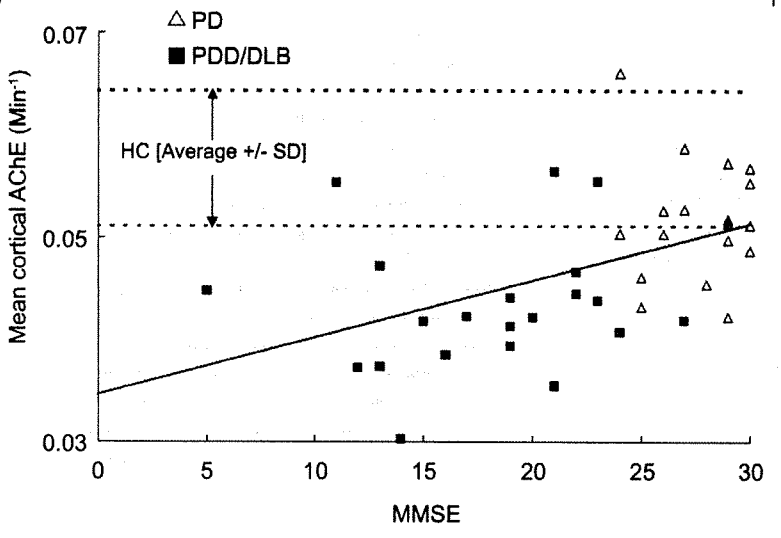

Correlation between MMSE scores and cortical k_3 values in Parkinson disease (PD: open triangles) and Parkinson disease with dementia/dementia with Lewy bodies (PDD/DLB: filled squares) ($r = 0.47$, $p < 0.005$). Cortical k_3 values are lower in PD and PDD/DLB than in healthy controls.

Patients with older onset PD, even without dementia, generally have significantly more cognitive problems compared to patients with younger onset. Therefore, it was interesting to compare patients with older onset PD with patients with younger onset PD since older onset PD might be different from younger onset PD in cholinergic pathology; however, we did not find any significant difference in brain AChE activity between the two groups.

Our third major finding was the widespread and profound reduction of AChE activity levels in the cerebral cortices, and especially in the posterior cortical regions, of patients with PDD and patients with DLB. These results are in agreement with previous PET studies on the same categories of patients,[14,15] and stand in contrast to our PET study on 14 patients with late-onset AD (age: 72 ± 4, MMSE score: 17.9 ± 3.5), among whom, using the same technique used in this study, we observed that AChE activity was reduced by only 13% on average.[24] Our PET technique shows substantial differences in the cholinergic profiles of AD and DLB, but it is premature to conclude that PET mapping of acetylcholinesterase could be used diagnostically.

We also directly compared the reduction in AChE activity in the PDD group with that in the DLB groups using SPM5, and found that there was no significant difference between them. Until now, there has been debate over whether PDD and DLB are one disease with different phenotypic expressions or two different diseases.[25] Our results suggest that DLB and PDD are essentially the same disease in terms of brain cholinergic dysfunction. The widespread and profound cerebral cortical cholinergic deficits associated with both may explain why cholinesterase inhibitors often bring about favorable responses in the treatment of dementia in both PDD and DLB.[1,8]

Our fourth major finding was that the decline in cerebral cortical AChE was more profound in patients with PDD/DLB than in patients with PD. Patients with PDD/DLB also exhibited a significant correlation between AChE activity in the cerebral cortex, especially in the posterior cingulate cortex (BA 31), and MMSE scores. These results confirm that brain cholinergic dysfunction significantly contributes to cognitive dysfunction in LBD. The most

significant difference in the degree of AChE activity reduction between the PDD/DLB group and the PD group occurred in the inferior temporal gyrus. In our study, subjects in the PDD/DLB group were older than those in the other two groups. We have previously reported, however, that k_3 values in the cerebral cortex, hippocampus, and amygdala are not influenced by aging.[26] As we expected, we did not observe any age effect on cortical k_3 values in HC in the present study, either, even though we performed SPM analysis with age as a covariate. Furthermore, we also performed the same analysis among age-matched groups (older HC, de novo early PD, early PD, advanced PD, PDD, and younger DLB groups), and we did not find any difference between results of age-matched groups and that of non-age-matched groups (HC, de novo early PD, early PD, advanced PD, PDD, and DLB groups).

ACKNOWLEDGMENT

The authors thank Y. Ogata (Faculty of Commerce, Chuo University, Tokyo, Japan) for evaluating cognitive functions in patients.

Received November 27, 2008. Accepted in final form March 30, 2009.

REFERENCES

1. Emre M, Arrsland D, Brown R, et al. Clinical diagnostic criteria for dementia associated with Parkinson's disease. Mov Disord 2007;22:1689–1707.
2. Hornykiewicz O, Kish SJ. Neurochemical basis of dementia in Parkinson's disease. Can J Neurol Sci 1984;11(1 suppl):185–190.
3. Kish SJ. Biochemistry of Parkinson's disease: is a brain serotonergic deficiency a characteristic of idiopathic Parkinson's disease? Adv Neurol 2003;91:39–49.
4. Bartus RT, Dean RL 3rd, Beer B, Lippa AS. The cholinergic hypothesis of geriatric memory dysfunction. Science 1982;217:408–414.
5. Perry E, Walker M, Grace J, Perry R. Acetylcholine in mind: a neurotransmitter correlate of consciousness? Trends Neurosci 1999;22:273–280.
6. Sarter M, Hasselmo ME, Bruno JP, Givens B. Unraveling the attentional functions of cortical cholinergic inputs: interactions between signal-driven and cognitive modulation of signal detection. Brain Res Rev 2005;48:98–111.
7. Whitehouse PJ, Hedreen JC, White CL 3rd, Price DL. Basal forebrain neurons in the dementia of Parkinson disease. Ann Neurol 1983;13:243–248.
8. McKeith IG, Dickson DW, Lowe J, et al. Consortium on DLB: diagnosis and management of dementia with Lewy bodies: third report of the DLB Consortium. Neurology 2005;65:1863–1872.
9. Perry EK, Haroutunian V, Davis KL, et al. Neocortical cholinergic activities differentiate Lewy body dementia from classical Alzheimer's disease. Neuroreport 1994;5:747–749.
10. Tiraboschi P, Hansen LA, Alford M, et al. Early and widespread cholinergic losses differentiate dementia with Lewy bodies from Alzheimer disease. Arch Gen Psychiatry 2002;59:946–951.
11. Namba H, Iyo M, Fukushi K, et al. Human cerebral acetylcholinesterase activity measured with positron emission tomography: procedure, normal values and effect of age. Eur J Nucl Med 1999;26:135–143.
12. Kuhl DE, Koeppe RA, Minoshima S, et al. In vivo mapping of cerebral acetylcholinesterase activity in aging and Alzheimer's disease. Neurology 1999;52:691–699.
13. Shinotoh H, Namba H, Yamaguchi M, et al. Positron emission tomographic measurement of acetylcholinesterase activity reveals differential loss of ascending cholinergic systems in Parkinson's disease and progressive supranuclear palsy. Ann Neurol 1999;46:62–69.
14. Bohnen NI, Kaufer DI, Ivanco LS, et al. Cortical cholinergic function is more severely affected in parkinsonian dementia than in Alzheimer disease: an in vivo positron emission tomographic study. Arch Neurol 2003;60:1745–1748.
15. Hilker R, Thomas AV, Klein JC, et al. Dementia in Parkinson disease: functional imaging of cholinergic and dopaminergic pathways. Neurology 2005;65:1716–1722.
16. Hughes AJ, Daniel SE, Kilford L, Lees AJ. Accuracy of clinical diagnosis of idiopathic Parkinson's disease: a clinico-pathological study of 100 cases. J Neurol Neurosurg Psychiatry 1992;55:181–184.
17. American Psychiatric Association. Diagnostic and Statistical Manual of Mental Disorders. 4th ed. Washington, DC: American Psychological Association; 2000.
18. Hobson DE, Lang AE, Martin WR, et al. Excessive daytime sleepiness and sudden-onset sleep in Parkinson disease: a survey by the Canadian Movement Disorders Group. JAMA 2002;287:455–463.
19. Herzog J, Volkmann J, Krack P, et al. Two-year follow-up of subthalamic deep brain stimulation in Parkinson's disease. Mov Disord 2003;18:1332–1337.
20. Folstein MF, Folstein SE, McHugh PR. "Mini-mental state": a practical method for grading the cognitive state of patients for the clinician. J Psychiatr Res 1975;12:189–198.
21. Meyer JH, Gunn RN, Myers R, Grasby PM. Assessment of spatial normalization of PET ligand images using ligand-specific templates. Neuroimage 1999;9:545–553.
22. Dotigny F, Ben Amor AY, Burke M, Vaucher E. Neuromodulatory role of acetylcholine in visually-induced cortical activation: Behavioral and neuroanatomical correlates. Neuroscience 2008;54:1607–1618.
23. Abe Y, Kachi T, Kato T. Occipital hypoperfusion in Parkinson's disease without dementia: correlation to impaired cortical visual processing. J Neurol Neurosurg Psychiatry 2003;74:419–422.
24. Shinotoh H, Namba H, Fukushi K, et al. Progressive loss of cortical acetylcholinesterase activity in association with cognitive decline in Alzheimer's disease: a positron emission tomography study. Ann Neurol 2000;48:194–200.
25. Aarsland D, Ballard CG, Halliday G. Are Parkinson's disease with dementia and dementia with Lewy bodies the same entity? J Geriatr Psychiatry Neurol 2004;17:137–145.
26. Namba H, Iyo M, Shinotoh H, Nagatsuka S, Fukushi K, Irie T. Preserved acetylcholinesterase activity in aged cerebral cortex. Lancet 1998;351:881–882.

Reduced perfusion in the anterior cingulate cortex of patients with pure autonomic failure: an ^{123}I-IMP SPECT study

S Hirano,[1] M Asahina,[1] Y Uchida,[2] H Shimada,[1] R Sakakibara,[2,3] H Shinotoh,[4] T Hattori[1]

[1] Department of Neurology, Graduate School of Medicine, Chiba University, Chiba, Japan; [2] Department of Radiology, Graduate School of Medicine, Chiba University, Chiba, Japan; [3] Department of Neurology, Toho University Sakura Medical Center, Chiba, Japan; [4] Asahi Hospital for Neurological Diseases, Chiba, Japan

Correspondence to: Dr S Hirano, Department of Neurology, Graduate School of Medicine, Chiba University, Chiba, Japan, 1-8-1 Inohana, Chuo-ku, Chiba, 260-8670, Japan; stimulus@mbf.ocn.ne.jp

Received 24 April 2008
Revised 17 July 2008
Accepted 26 September 2008

ABSTRACT

Background: Pure autonomic failure (PAF) is a selective peripheral disorder in which Lewy bodies form within the autonomic ganglia. Patients with this disorder usually have no central lesions; however, chronic autonomic failure may secondarily affect the central nervous system. This study evaluated brain perfusion in patients with PAF by using N-isopropyl-p-^{123}I iodoamphetamine (^{123}I-IMP) single photon emission computed tomography (SPECT).

Methods: Six patients with PAF (all men; mean (SD) age 68 ± 5 years) who had experienced autonomic symptoms for more than 5 years and six age-matched healthy control subjects (all men; mean (SD) age 67 ± 5 years) were included in this study. The regions of interest (ROI) on spacially normalized ^{123}I-IMP SPECT images were automatically computed for both groups.

Results: Perfusion of the dorsal anterior cingulate cortex was decreased in the PAF group compared with the healthy control group (0.93 vs 1.01; $p<0.001$). In the other brain regions measured, there was no significant difference in regional perfusion between the two groups.

Conclusions: The dorsal anterior cingulate cortex is poorly perfused and may be functionally altered in patients with PAF. The reduced perfusion in such individuals may be a secondary change that results from chronic autonomic failure.

Pure autonomic failure (PAF) is an idiopathic sporadic neurodegenerative disorder that presents with clinical symptoms of autonomic dysfunction (e.g. orthostatic hypotension, defective sweating and urogenital dysfunction) but no other neurological deficits (i.e. motor, sensory, extrapyramidal or cerebellar symptoms).[1] The main autonomic symptom in patients with PAF is orthostatic hypotension, which is the result of an inability to activate sympathetic pathways to cause vasoconstriction during gravitational challenges. The main structure affected in PAF is the sympathetic ganglionic neurons, where Lewy body pathology has been documented. Neurodegenerative diseases with Lewy body pathology include not only PAF but also Parkinson disease (PD) and dementia with Lewy bodies (DLB).

Recently, automated voxel-by-voxel statistical analysis using three-dimensional stereotactic surface projection (3D-SSP) has made it possible to semi-quantitatively evaluate regional cerebral blood flow (rCBF) in single photon emission computed tomography (SPECT) images.[2] Studies that used this technique have revealed that rCBF is decreased in the occipital lobe both in PD patients with dementia[3] and in patients with DLB,[4] although rCBF studies have been inconclusive in patients with PD who do not have dementia. As far as we know, there has been no brain perfusion SPECT study of patients with PAF. Although the main affected structure in patients with PAF is the sympathetic autonomic ganglia, such individuals may have reduced perfusion in the brain similar to that seen in patients with PD or DLB, diseases that share underlying Lewy body pathology. Meanwhile, PD and DLB patients may also exhibit autonomic failure, but it is often less severe than that of PAF patients. Post-synaptic sympathetic denervation may influence the central autonomic nervous system via afferent feedback and may modulate rCBF.

We used SPECT and N-isopropyl-p-^{123}I iodoamphetamine (^{123}I-IMP) followed by automated ROI analysis with 3D-SSP to evaluate rCBF in patients with PAF, which we then compared with that in age-matched healthy volunteers in order to elucidate the brain region of hypoperfusion in PAF.

METHODS

Participants

This study included six patients with PAF (all male; mean (SD) age 68 ± 5 years; mean (SD) disease duration 8.5 ± 3.6 years). ^{123}I-IMP brain SPECT data for these individuals were retrospectively collected from a PAF database of 13 patients. The six patients with PAF had all had orthostatic hypotension and dysautonomia for over 5 years, without clinical evidence of nonautonomic pathology or central neurological degeneration (e.g. cerebellar signs or parkinsonism). Brain MRI was performed in all PAF patients and showed that none had marked ischemic changes nor any specific changes indicating the presence of a neurodegenerative disorder. Mild white matter changes, however, were found in two of the six patients. Control subjects were six age-matched healthy volunteers (all male; mean (SD) age 67 ± 5 years). SPECT study of healthy volunteers was approved by the Ethics Committee of Chiba University Hospital, with written consent obtained from the patient prior to the procedure. Autonomic function tests were performed only in patients with PAF.

Autonomic tests

The 70° head-up tilt test was performed with blood pressure and heart rate automatically recorded at 1-minuite intervals by a sphygmomanometer. Electrocardiogram R–R intervals with an accuracy of 1 msec were recorded with the patient in the supine position and breathing normally, and the coefficients of variation of the R–R interval were calculated. Venous blood was collected after at least 20 minutes of rest in the supine position in order to measure plasma norepinephrine levels (normal: >100 pg/ml).

Table 1 The demography, autonomic test results and regional cerebral blood flow values of patients with pure autonomic failure and age-matched healthy controls

	Healthy controls	Patients with PAF	Difference between controls and PAF group (%)
	Mean (SD)	Mean (SD)	
Plasma noradrenaline (pg/ml)	-	121 (100)	-
Head-up tilt test	-		-
Systolic BP change (mm Hg)	-	71 (20)	-
Diastolic BP change (mm Hg)	-	42 (12)	-
Heart rate change (beats/min)	-	5 (11)	-
R–R interval coefficient of variance (%)	-	0.95 (0.22)	-
Postmicturition residual (ml)	-	109 (88)	-
^{123}I-IMP SPECT			
Frontal cortex	1.01 (0.02)	1.00 (0.05)	−1.75
Ventral anterior cingulate cortex	0.96 (0.06)	0.88 (0.03)	−8.43
Dorsal anterior cingulate cortex	1.01 (0.01)	0.93 (0.01)*	−7.93
Posterior cingulate cortex	1.05 (0.06)	1.00 (0.06)	−4.78
Parietal cortex	0.99 (0.02)	1.01 (0.06)	+1.41
Temporal cortex	0.98 (0.02)	0.97 (0.08)	−0.72
Occipital cortex	1.02 (0.04)	1.02 (0.06)	−0.26
Thalamus	1.17 (0.07)	1.10 (0.04)	−6.06
Midbrain	1.00 (0.04)	0.96 (0.06)	−4.78
Pons	0.98 (0.04)	0.94 (0.10)	−3.78
Cerebellum	0.99 (0.04)	0.99 (0.09)	+0.08

Regional cerebral blood flow values are normalised to the whole cortex (reference region).
*$p<0.001$, compared with healthy controls. BP, blood pressure; PAF, pure autonomic failure.

The urodynamic tests performed comprised measurement of postmicturition residuals, urethral pressure profilometry and water cystometry. Twenty-four-hour blood pressure monitoring was performed in five of the patients with PAF.

Single photon emission computed tomography All participants received 111 MBq of ^{123}I-IMP injected intravenously in resting condition. Data acquisition was initiated 30 minutes after injection using a three-headed gamma camera PRISM 3000 XP (Shimadzu, Kyoto, Japan) equipped with fan-beam collimators. Participants were scanned in the supine position in a calm place. The SPECT data were obtained in a 128 x 128 matrix, slice thickness 2.16 mm, in 24 steps with 60 seconds for each step. All images were reconstructed with a Butterworth filter (cut-off frequency 0.39 cycle/cm, order 4), resulting in a resolution of approximately 13 mm at full width, which was half the maximum at the centre of rotation. The reconstructed pixel size was 2.16 mm. Attenuation was corrected using Chang's technique.[5]

The iSSP3 software (Nihon Medi-physics Co., Ltd, Hyogo, Japan) and an Odyssey VP processing computer were used for 3D-SSP analysis. Methods for 3D-SSP analysis have been previously described in detail by Minoshima *et al*.[2] Each image was evaluated by ROI analysis and placed on a normalised template image by using stereotactic extraction estimation software[6] on a Windows XP PC. The ROI identified were: the frontal, temporal, parietal and occipital cortices; the midbrain; the pons; the cerebellum; the ventral anterior cingulate cortex (ACC); the dorsal ACC; and the posterior cingulate cortex. rCBF values were normalised with respect to the whole cortex (reference region). rCBF values were compared between healthy subjects and the PAF group by unpaired Student t-tests. Using Bonferroni's correction, the p value was adjusted to 0.005 (two-tailed), which was chosen as the significance threshold to avoid errors due to the multiplicity of statistical analysis.

RESULTS

The demography and rCBF ratio value of the six patients with PAF is shown in Table 1. In the head-up tilt test, all six PAF patients exhibited severe orthostatic hypotension (minimum systolic/diastolic blood pressure change: 46/25 mm Hg). The patients with PAF showed reduced R–R interval coefficients of variation (mean (SD): 0.95±0.22%; lower limit of healthy in seventh decade Japanese controls: 1.25%),[7] suggesting cardiac parasympathetic dysfunction. Plasma norepinephrine levels in the resting supine state were low (<100 pg/ml) in four of the six patients with PAF. Twenty-four-hour blood pressure monitoring revealed nocturnal hypertension (systolic/diastolic blood pressure >140/110 mm Hg) in all five patients with PAF who were examined. Four of the six PAF patients showed detrusor hyperactivity, suggestive of central dysregulation in those patients.

rCBF was significantly reduced in the dorsal ACC (−7.9%; $p<0.001$) and nonsignificantly reduced in the ventral ACC (−8.43%; $p<0.05$) in patients with PAF compared with healthy control subjects. rCBF in no other evaluated region—including the occipital cortex, brainstem and cerebellum—varied significantly between patients with PAF and healthy controls. When each region was assessed individually, the dorsal ACC was the only region for which rCBF measurements from all PAF patients were more than two standard deviations less than normal mean. Figure 1 shows ^{123}I-IMP SPECT images of each PAF patient analysed with 3D-SSP. The coloured areas in the images represent the regions where perfusion was decreased. Most patients with PAF showed reduced perfusion in the ACC and the medial frontal lobe compared with the healthy controls.

DISCUSSION

In this study, we were able to show reduced perfusion of the ACC in patients with PAF. The 3D-SSP methodology we used does not permit analysis of deep brain regions such as the striatum, globus pallidum and insula. Nonetheless, this voxel-based automated brain analysis provided clear objective data regarding most of the cerebral cortex, the thalamus, the brain stem and the cerebellum.

Another study that used voxel-based morphometric analysis in patients with PAF showed reduced grey matter volume in the ACC and insular cortex.[8] The authors suggested that a poverty

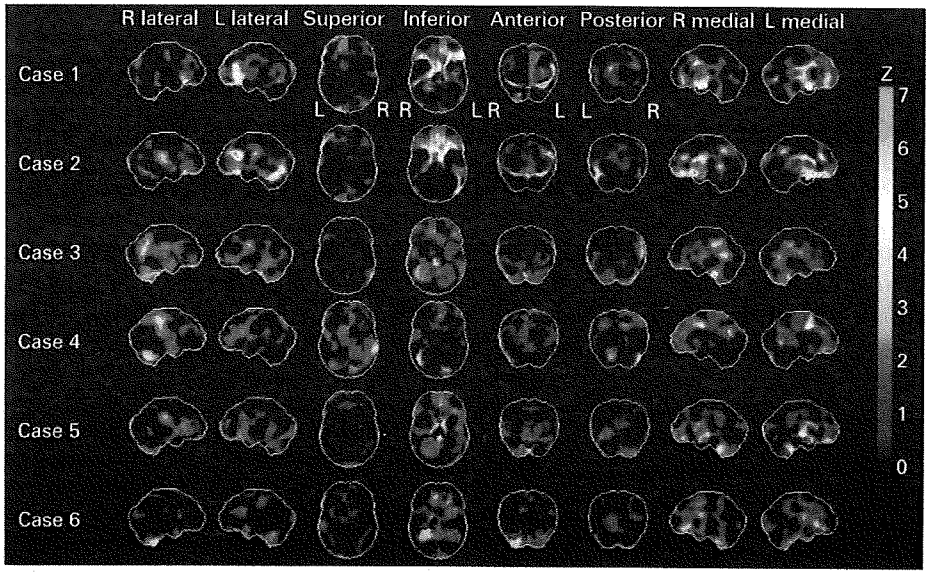

Figure 1 N-isopropyl-p-[123]I iodoamphetamine single photon emission computed tomography images of six patients with pure autonomic failure. The images were generated by three-dimensional stereotactic surface projection analysis (Z map) and were normalised using global scaling. Red regions show the areas with the lowest perfusion. Individual images were compared with images from with age-matched healthy controls. Most PAF patients show reduced perfusion in cingulate cortex and medial frontal lobe. L, left; R, right.

of afferent information in patients with PAF results in reduced functional representation of autonomic states and the consequent adaptation of the ACC. The 3D-SSP method minimises partial volume effect by extracting brain cortex data tangentially from the brain surface, although the atrophy effect can not be excluded completely.[9] Nonetheless, we did not detect overt brain atrophy in the PAF cohort.

The ACC has an important role in controlling cardiovascular function.[10] Our PAF patients had severe cardiovascular autonomic failure, manifest as orthostatic hypotension and nocturnal (recumbent) hypertension. Frequent hypoperfusion due to orthostatic hypotension in the brain or other organs may have influenced neural activities in the ACC in our patients via peripheral and/or central feedback mechanisms. Alternatively, chronic nocturnal hypertension may have contributed to the reduced perfusion in ACC, which is vulnerable in hypertensive subjects.[11] On the other hand, the ACC is involved in the perception of changes in bladder volume and is probably has a role in the modulation of bladder control.[12] ACC perfusion in patients with PAF could be secondarily affected by the absence of neuronal activity resulting from the perception of bladder filling.

PAF is considered to belong in the spectrum of Lewy body diseases, which also includes PD and DLB. Lewy body pathology has been observed in the cerebral cortex of patients with PAF,[13] and some PAF cases evolve clinically into PD or DLB.[14 15] ACC hypoperfusion in our patients might, therefore, reflect Lewy body pathology. However, Lewy bodies are not restricted to the cingulate cortex.[13] Patients with PD, as well as those with PAF, frequently present with post-synaptic sympathetic lesions. Matsui *et al.*[16] demonstrated using 3D-SSP analysis that PD patients with orthostatic hypotension showed ACC hypoperfusion compared with patients without orthostatic hypotension. Their findings indicate that cingulate cortex hypoperfusion is related to chronic sympathetic failure rather than to central Lewy body pathology.

In conclusion, the ACC is poorly perfused and may be functionally altered in patients with PAF. The ACC has a role in highest-level autonomic control in humans and its reduced perfusion may reflect secondarily altered central autonomic activity due to chronic autonomic failure.

Acknowledgements: Thanks to Dr Akira Katagiri and Dr Setsu Sawai for data collection.

Competing interests: None.

REFERENCES

1. **Bannister R,** Mathias CJ. Clinical features and evaluation of the primary chronic autonomic failure syndromes. In: Bannister R, ed. *Autonomic failure. A textbook of clinical disorders of the autonomic nervous system.* 4 ed. Oxford: Oxford University Press, 1999: 307–16.
2. **Minoshima S,** Koeppe RA, Frey KA, *et al.* Stereotactic PET atlas of the human brain: aid for visual interpretation of functional brain images. *J Nucl Med* 1994;**35**:949–54.
3. **Abe Y,** Kachi T, Kato T, *et al.* Occipital hypoperfusion in Parkinson's disease without dementia: correlation to impaired cortical visual processing. *J Neurol Neurosurg Psychiatry* 2003;**74**:419–22.
4. **Kasama S,** Tachibana H, Kawabata K, *et al.* Cerebral blood flow in Parkinson's disease, dementia with Lewy bodies, and Alzheimer's disease according to three-dimensional stereotactic surface projection imaging. *Dement Geriatr Cogn Disord* 2005;**19**:266–75.
5. **Chang L.** A method for attenuation correction in radionuclide computed tomography. *IEEE Trans Nucl Sci* 1978;**25**:638–43.
6. **Mizumura S,** Kumita S, Cho K, *et al.* Development of quantitative analysis method for stereotactic brain image: assessment of reduced accumulation in extent and severity using anatomical segmentation. *Ann Nucl Med* 2003;**17**:289–95.
7. **Fujimoto J,** Hirota M, Hata M, *et al.* Normal reference values and prediction equation of autonomic nerve functions based on variations in the R–R interval in electrocardiographs. *J Japan Diab Soc* 1987;**30**:167–73 (Japanese).
8. **Critchley HD,** Good CD, Ashburner J, *et al.* Changes in cerebral morphology consequent to peripheral autonomic denervation. *NeuroImage* 2003;**18**:908–16.
9. **Pirson A,** Vander Borght T. Age and gender effects on normal regional cerebral blood flow. *AJNR* 2006;**27**:1161–3.
10. **Critchley HD.** Neural mechanisms of autonomic, affective, and cognitive integration. *J Comp Neurol* 2005;**493**:154–66.
11. **Beason-Held LL,** Moghekar A, Zonderman AB, *et al.* Longitudinal changes in cerebral blood flow in the older hypertensive brain. *Stroke* 2007;**38**:1766–73.
12. **Blok BF,** Willemsen AT, Holstege G. A PET study on brain control of micturition in humans. *Brain* 1997;**120**:111–21.
13. **Terao Y,** Takeda K, Sakuta M, *et al.* Pure progressive autonomic failure: A clinicopathological study. *Eur Neurol* 1993;**33**:409–15.
14. **Kaufmann H,** Nahm K, Purohit D, *et al.* Autonomic failure as the initial presentation of Parkinson disease and dementia with Lewy bodies. *Neurology* 2004;**63**:1093–5.
15. **Yamanaka Y,** Asahina M, Hiraga A, *et al.* Over 10 years of isolated autonomic failure preceding dementia and Parkinsonism in 2 patients with Lewy body disease. *Mov Disord* 2007;**22**:595–7.
16. **Matsui H,** Udaka F, Miyoshi T, *et al.* Three-dimensional stereotactic surface projection study of orthostatic hypotension and brain perfusion image in Parkinson's disease. *Acta Neurol Scand* 2005;**112**:36–41.

Estimation of Plasma IC_{50} of Donepezil for Cerebral Acetylcholinesterase Inhibition in Patients With Alzheimer Disease Using Positron Emission Tomography

Tsuneyoshi Ota, PhD, MD,† Hitoshi Shinotoh, PhD, MD,*‡ Kiyoshi Fukushi, PhD,* Tatsuya Kikuchi, PhD,* Koichi Sato, PhD, MD,*§ Noriko Tanaka, PhD, MD,*|| Hitoshi Shimada, PhD, MD,*¶ Shigeki Hirano, PhD, MD,*# Michie Miyoshi, MD,* Heii Arai, PhD, MD,† Tetsuya Suhara, PhD, MD,* and Toshiaki Irie, PhD**

Objectives: Estimate the value of in vivo plasma IC_{50} of donepezil, the concentration of donepezil in plasma that inhibits brain acetylcholinesterase (AChE) activity by 50% at the steady-state conditions of donepezil between the plasma and the brain.

Methods: *N*-[^{11}C] methylpiperidin-4-*yl* acetate ([^{11}C]MP4A) positron emission tomography was performed in 16 patients with probable Alzheimer disease (AD) before and during the treatment of donepezil (5 mg/day) with a mean interval of 5.3 months. The plasma IC_{50} value of donepezil was estimated from plasma donepezil concentrations and cerebral cortical mean AChE inhibition rates measured by positron emission tomography, using one-parameter model.

Results: Donepezil reduced AChE activity uniformly in the cerebral cortex compared with the baseline in each AD patient, and the mean reduction rate in the cerebral cortex was 34.6%. The donepezil concentrations in the plasma ranged from 18.5 to 43.9 ng/mL with a mean of 28.9 ± 7.3 ng/mL. The plasma IC_{50} value was estimated to be 53.6 ± 4.0 ng/mL.

Conclusions: Once the plasma IC_{50} of donepezil is determined, the brain AChE inhibition rate could be estimated from the plasma concentration of donepezil in each subject based on the plasma IC_{50}. Now that the mean donepezil concentrations in the plasma, when the patients took 5 mg/day, remained 28.9 ng/mL, approximately half of the plasma IC_{50}, higher dose of donepezil might provide further benefits for patients with AD. This technique can be also applied to measure the in vivo plasma IC_{50} of other cholinesterase inhibitors such as rivastigmine and galantamine.

Key Words: acetylcholinesterase, Alzheimer disease, donepezil, in vivo plasma IC_{50}, positron emission tomography

(*Clin Neuropharm* 2009;00: 00–00)

Donepezil hydrochloride, a specific acetylcholinesterase (AChE) inhibitor, is widely used for the treatment of Alzheimer disease (AD). Donepezil inhibits AChE and increases concentrations of acetylcholine in the synaptic cleft. This is believed to contribute to the cognitive improvement in patients with AD during treatment with donepezil.[1] Donepezil has also come to be more expected as a disease-modifying drug.[2–4] Until recently, patients with AD in Japan were treated with an identical dose (5 mg/day). Now that 10 mg of donepezil is also permitted in Japan, the decision of the appropriate clinical dosage of donepezil is necessary.

N-[^{11}C]methylpiperidin-4-*yl* acetate ([^{11}C]MP4A or AMP) and *N*-[^{11}C]methylpiperidin-4-*yl* propionate ([^{11}C]MP4P or PMP) are both acetylcholine analogues which were developed as positron emission tomography (PET) radiotracers for brain AChE mapping[5,6]; they have been applied to the quantification of cortical AChE activity in healthy subjects[7,8] and in patients with AD and other neurodegenerative disorders.[9–11] Both radiotracers have also been used to evaluate the inhibitory effects of donepezil on brain AChE activity in patients with AD[12–15] and in monkeys.[16,17]

Recently, the correlation between plasma galantamine concentrations and brain AChE inhibition rates was examined in patients with AD using [^{11}C]MP4P.[18] As for donepezil, however, there has been no in vivo human study on the quantitative correlation between the plasma donepezil concentrations and brain AChE inhibition rates. We investigated the correlation between plasma donepezil concentrations and AChE inhibition rates in the cerebral cortex using [^{11}C]MP4A PET in patients with probable AD before and during treatment. We also estimated in vivo plasma IC_{50} of donepezil, on the premise that the inhibitory effects of AChE inhibitors are dose dependent on AChE activity.[17,19] Subsequently, the AChE inhibition rates in the cerebral cortex can be estimated from the plasma concentration of donepezil in each patient with AD at various doses. This is the first report on the estimation of in vivo plasma IC_{50} of donepezil in patients with AD.

This study is an extension of the previous study in which we quantitatively measured cerebral cortical AChE activities in 3 patients with AD once before and once during donepezil treatment by [^{11}C]MP4A PET and showed that donepezil reduced AChE activity in the cerebral cortex by 39 ± 5%.[13]

PATIENTS AND METHODS

Subjects

Sixteen patients (5 men and 11 women ranging from 50 to 83 years old) with AD participated in this study. The patients' mean age was 66.0 ± 10.2 years, and the mean duration of illness was 2.7 ± 1.4 years at the time of the baseline PET study. The mean duration of treatment was 5.3 ± 2.0 months. Three patients with AD included in the previous report were also included in this study.[13] The patients had been taking neither anticholinergic

From the *Department of Molecular Probe, Molecular Imaging Center, National Institute of Radiological Sciences, Chiba; †Department of Psychiatry, Juntendo University School of Medicine, Tokyo; ‡Asahi Hospital for Neurological Diseases; §Department of Psychiatry, Teikyo University Chiba Medical Center; ||Department of Neurosurgery, Tokyo Women's Medical University Medical Center East, Tokyo; ¶Department of Neurology, Chiba University School of Medicine, Chiba; and #Department of Neurology, JR Tokyo General Hospital, Tokyo, Japan.

Address correspondence and reprint requests to Tsuneyoshi Ota, PhD, MD, Department of Psychiatry, Juntendo University School of Medicine, Tokyo, Japan; E-mail: ota@juntendo.ac.jp

There was no funding sponsor for this study.

DOI: 10.1097/WNF.0b013e3181c71be9